Design, Synthesis, and Biological Activity of Boronic Acid-Based Histone Deacetylase Inhibitors

Nobuaki Suzuki,[†] Takayoshi Suzuki,*[,†] Yosuke Ota,[†] Tatsuya Nakano,[‡] Masaaki Kurihara,[§] Haruhiro Okuda,[§] Takao Yamori,[#] Hiroki Tsumoto,[†] Hidehiko Nakagawa,[†] and Naoki Miyata*[,†,§]

Graduate School of Pharmaceutical Sciences, Nagoya City University, 3-1 Tanabe-dori, Mizuho-ku, Nagoya, Aichi 467-8603, Japan, Division of Medicinal Safety Science, National Institute of Health Sciences, 1-18-1 Kamiyoga, Setagaya-ku, Tokyo 158-8501, Japan, Division of Organic Chemistry, National Institute of Health Sciences, 1-18-1 Kamiyoga, Setagaya-ku, Tokyo 158-8501, Japan, and Division of Molecular Pharmacology, Cancer Chemotherapy Center, Japanese Foundation for Cancer Research, 3-10-6 Ariake, Koto-ku, Tokyo 135-8550, Japan

Received February 2, 2009

Guided by the proposed catalytic mechanism of histone deacetylases (HDACs), we designed and synthesized a series of boronic acid-based HDAC inhibitors bearing an α-amino acid moiety. In this series, compounds (*S*)-**18**, **20**, and **21** showed potent HDAC-inhibitory activity, highlighting the significance of the (*S*)-amino acid moiety. In cancer cell growth inhibition assays, compounds (*S*)-**18**, **20**, and **21** exerted strong activity, and the values of the ratio of the concentration causing 50% growth inhibition (GI_{50}) to the concentration causing 50% enzyme inhibition (IC_{50}), i.e., GI_{50}/IC_{50}, were low. The potency of these compounds was similar to that of clinically used suberoylanilide hydroxamic acid (SAHA) (**2**). The results of Western blot analysis indicated that the cancer cell growth-inhibitory activity of compounds (*S*)-**18**, **20**, and **21** is the result of HDAC inhibition. A molecular modeling study suggested that the hydrated boronic acid interacts with zinc ion, Tyr residue, and His residue in the active site of HDACs. Our findings indicate that these boronic acid derivatives represent an entry into a new class of HDAC inhibitors.

Introduction

The acetylation status of lysine residues in nucleosomal histones is tightly controlled by two counteracting enzyme families, the histone acetyl transferases and the histone deacetylases (HDACs[a]).[1] The latter family can be divided into two categories: Zn^{2+}-dependent enzymes and NAD^+-dependent enzymes.[2] The Zn^{2+}-dependent HDACs are closely connected with control of gene expression and cell cycle progression.[3] The inhibition of HDACs causes histone hyperacetylation and leads to transcriptional activation of genes such as $p21^{WAF/CIP1}$, Gadd 45, FAS, and caspase-3, which are associated with growth arrest and apoptosis in tumor cells.[4] Indeed, HDAC inhibitors, such as trichostatin A (TSA, **1**),[5] suberoylanilide hydroxamic acid (SAHA, also known as vorinostat, **2**),[6] PXD-101 (**3**),[7] and MS-275 (**4**)[8] (Chart 1), have been reported to inhibit cell growth, induce terminal differentiation in tumor cells, and prevent the formation of malignant tumors, and they have been developed as antitumor agents. Among them, SAHA has recently been approved by the FDA for treatment of cutaneous T-cell lymphoma. In addition, there are several lines of evidence indicating that HDAC inhibitors are effective as therapeutic agents for other diseases, including inflammation and neurodegenerative diseases.[9] Moreover, it has recently been reported that HDAC inhibitors, such as TSA (**1**), SAHA (**2**), and valproic acid, improve the efficiency of induction of pluripotent stem cells without introduction of the oncogene c-Myc, suggesting the importance of HDAC inhibitors in regenerative medicine.[10] Consequently, there are many ongoing research programs to find more potent and selective HDAC inhibitors.[11]

To date, X-ray crystal structures of human HDAC4,[12] HDAC7,[13] HDAC8,[14] and archaebacterial HDAC-like protein (HDLP)[15] have been published. A number of potent and selective inhibitors have been identified by structure-based drug design using these crystal structures.[11] Recently, the catalytic mechanism of the deacetylation of acetylated lysine substrates by HDACs was proposed, based on a density functional theory QM/MM study of HDLP,[16] and this also offers many clues for the design of HDAC inhibitors. Herein we report the synthesis and biological activity of boronic acid-based HDAC inhibitors, which were designed on the basis of the proposed catalytic mechanism of HDACs.

Chemistry

Compounds **5**−**26** prepared for this study are shown in Tables 1−3. The routes used for the synthesis of the compounds are shown in Schemes 1−5. Scheme 1 shows the preparation of α-amino acid derivatives **5**−**10**. These compounds were synthesized from diethyl aminomalonate **27**. Compound **27** was treated with $(Boc)_2O$ to yield *N*-Boc compound **28**. Compound **28** was allowed to react with 5-bromopent-1-ene in the presence of NaOEt in refluxing EtOH to give C-alkylated compound **29**. Hydrolysis of the ethyl ester of **29** with an equivalent amount of LiOH gave monocarboxylic acid **30**, and subsequent decarboxylation reaction afforded α-amino acid derivative **31**. Compound **31** was hydrolyzed with LiOH followed by treatment with an appropriate aromatic amine in the presence of EDCI and HOBt to give amides **33**−**38**. The hydroboration reaction of amides **33**−**38** with pinacolborane using $[Ir(cod)Cl]_2$ catalyst and dppm or dppe ligand gave terminal boronic esters **39**−**44**.[17] Hydrolysis of the boronic esters **39**−**44** using NH_4OAc and $NaIO_4$ in acetone−water yielded boronic acids **5**−**10**.[18]

Scheme 2 shows the preparation of boronic acids **11**−**16**, in which the α-amino moiety of compounds **5**−**10** was removed.

* To whom correspondence should be addressed. For T.S.: phone and fax, +81-52-836-3407; e-mail, suzuki@phar.nagoya-cu.ac.jp. For N.M.: phone and fax, +81-52-836-3407; miyata-n@phar.nagoya-cu.ac.jp.

[†] Nagoya City University.

[‡] Division of Medicinal Safety Science, National Institute of Health Sciences.

[§] Division of Organic Chemistry, National Institute of Health Sciences.

[#] Japanese Foundation for Cancer Research.

[a] Abbreviations: HDAC, histone deacetylase; TSA, trichostatin A; SAHA, suberoylanilide hydroxamic acid; HDLP, HDAC-like protein.

10.1021/jm900125m CCC: $40.75
Published on Web 04/14/2009

Chart 1. Examples of HDAC Inhibitors

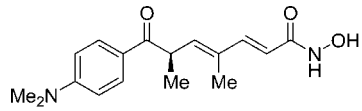

1

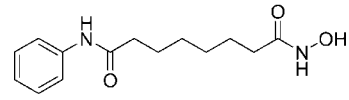

2

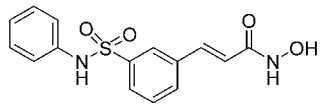

3

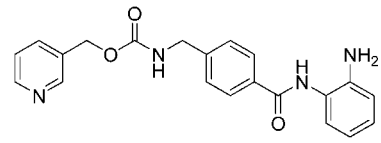

4

Scheme 1[a]

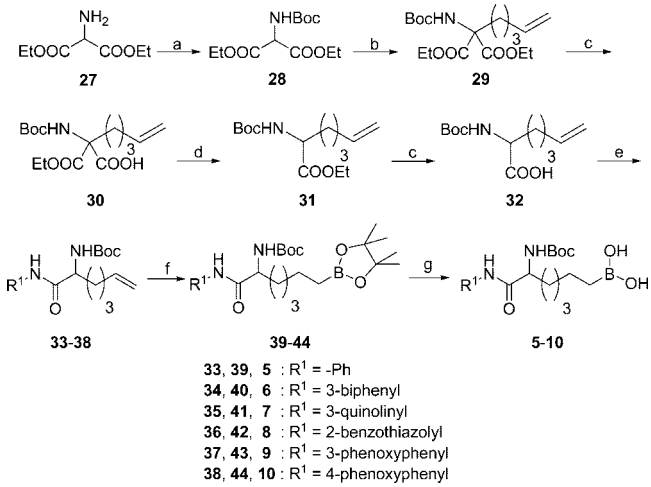

[a] Reagents and conditions: (a) $(Boc)_2O$, Et_3N, THF, room temp, 81%; (b) NaOEt, 5-bromopent-1-ene, EtOH, reflux, 89%; (c) $LiOH \cdot H_2O$, EtOH, H_2O, 0 °C, 94% for **32**, 99% for **30**; (d) toluene, reflux, 94%; (e) R^1-NH_2, 1-ethyl-3-(3-dimethylaminopropyl)carbodiimide (EDCI), 1-hydroxybenzotriazole hydrate ($HOBt \cdot H_2O$), DMF, room temp, 67−95%; (f) $[Ir(cod)Cl]_2$, bis(diphenylphosphino)methane (dppm) or 1,2-bis(diphenylphosphino)ethane (dppe), pinacolborane, CH_2Cl_2, room temp, 32−93%; (g) NH_4OAc, $NaIO_4$, acetone, H_2O, room temp, 10−92%.

These compounds were synthesized from hept-6-enoic acid **45** using the same synthetic approach as described for compounds **5**−**10**.

Scheme 3 shows the preparation of α-amino acid derivatives **17**−**24**, in which the Boc group of **6** was replaced with various carbonyl moieties. These compounds were prepared from **40** in three steps: deprotection of the Boc group, condensation with an appropriate aromatic carboxylic acid, and hydrolysis of the boronic esters.

Scheme 4 shows the preparation of malonic acid derivatives **25** and **26**, in which the α-aminocarbonyl moiety of compounds **18** and **20** was replaced with the corresponding carboxamide. These compounds were synthesized from *tert*-butyl ethyl malonate **66**. Treatment of **66** with 5-bromopent-1-ene in the presence NaH in THF yielded compound **67**. The ethyl ester of **67** was hydrolyzed with an equivalent amount of LiOH, followed by condensation with biphenyl-3-ylamine to give amide **69**. Hydroboration, deprotection of *tert*-butyl ester using TFA, condensation with an appropriate aromatic amine, and hydrolysis of the boronic ester gave the malonic acid derivatives **25** and **26**.

Scheme 5 shows the preparation of optically active α-amino acid derivatives (*S*)- and (*R*)-**18**, **20**, **21**. These compounds were synthesized using the procedure reported by Nishino and coworkers.[19] Compound (*RS*)-**31** was subjected to the action of subtilisin from *Bacillus licheniformis* in a mixture of DMF and water to yield (*S*)-**32** as a white solid. The recovered (*R*)-**31** was hydrolyzed with LiOH to afford (*R*)-**32**. The synthesis of (*S*)- and (*R*)-**18**, **20**, **21** was accomplished from (*S*)-**32** or (*R*)-**32** using the procedure described for the synthesis of α-amino acid derivatives (shown in Schemes 1 and 3). The enantiomeric excess of (*S*)- and (*R*)-**18**, **20**, **21** was determined to be >95% by chiral column chromatography.

Results and Discussion

Drug Design. In 1999, Finnin et al. reported X-ray crystal structures of HDLP complexed with inhibitors.[15] The enzyme contains a zinc ion at the bottom of the active site, and the active center consists of a tyrosine, two aspartic acids, and three histidines. In 2006, Corminboeuf et al. carried out density functional theory QM/MM studies on the deacetylation reaction catalyzed by HDLP.[16] The proposed mechanism suggested by the calculation results is depicted in Figure 1a. In this mechanism, the carbonyl oxygen of the substrate binds the zinc ion and is located adjacent to a water molecule. The electrophilicity of the carbonyl carbon is increased by coordination to the zinc ion, and so the carbonyl carbon is attacked by the water molecule activated by His 140 and His 141 (HDAC1 numbering). This nucleophilic attack results in a tetrahedral transition state, which is stabilized by a zinc−oxygen interaction and by hydrogen bonds with Tyr 303 and His 140. In the final step, proton transfer from His 141 to the nitrogen of the intermediate triggers scission of the carbon−nitrogen bond to afford the acetate and lysine products.

In designing selective HDAC inhibitors, we focused on the proposed deacetylation mechanism. On the basis of this mechanism, we designed α-amino acid derivatives **A** (Figure 1b) in which the acetamide of the acetylated lysine substrate is replaced by boronic acid. Because the boron atom of the boronic acids **A** has a vacant p-orbital, it could be attacked by a water molecule in the active site. The generated boronic acid−H_2O "ate" complex could act as a transition state analogue of the deacetylation of acetylated lysine substrates. That is, the hydrated boronic acid would bind the zinc ion and form two hydrogen bonds with Tyr 303 and His 140, which would lead to HDAC inhibition.

Enzyme Assays. In our exploratory study on boronic acid-based HDAC inhibitors, we initially focused on the R^1 group (Table 1 and Supporting Information Figure S1). We chose various aromatic rings as the R^1 group because we had already discovered that thiolate compounds bearing aromatic groups such as phenyl, 3-biphenyl, and 3-quinolinyl potently inhibited HDACs both in enzyme assays and in cellular assays.[11] Boronic

Scheme 2[a]

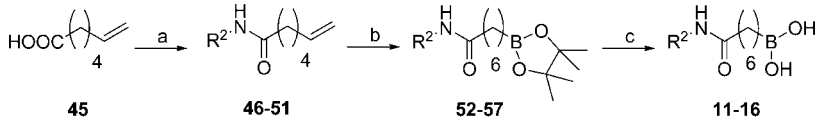

45 **46-51** **52-57** **11-16**

46, **52**, **11** : R^2 = -Ph
47, **53**, **12** : R^2 = 3-biphenyl
48, **54**, **13** : R^2 = 3-quinolinyl
49, **55**, **14** : R^2 = 2-benzothiazolyl
50, **56**, **15** : R^2 = 3-phenoxyphenyl
51, **57**, **16** : R^2 = 4-phenoxyphenyl

[a] Reagents and conditions: (a) R^2-NH_2, EDCI, HOBt, DMF, room temp, 72−95%; (b) $[Ir(cod)Cl]_2$, dppm or dppe, pinacolborane, CH_2Cl_2, room temp, 13−74%; (c) NH_4OAc, $NaIO_4$, acetone, H_2O, room temp, 35−94%.

Scheme 3[a]

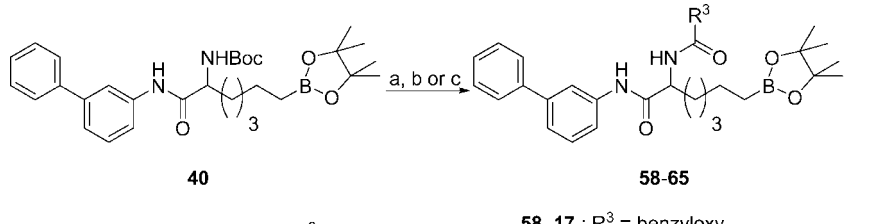

40 **58-65**

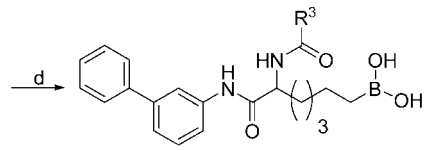

17-24

58, **17** : R^3 = benzyloxy
59, **18** : R^3 = -Ph
60, **19** : R^3 = 4-(*N,N*-dimethylamino)phenyl
61, **20** : R^3 = 3-pyridinyl
62, **21** : R^3 = 5-thiazolyl
63, **22** : R^3 = 4-thiazolyl
64, **23** : R^3 = 2-indolyl
65, **24** : R^3 = 2-quinolinyl

[a] Reagents and conditions: (a) HCl, AcOEt, $CHCl_3$, room temp, 100%; (b) R^3-COOH, EDCI, HOBt, DMF, room temp, 11−100%; (c) R^3-COCl, Et_3N, CH_2Cl_2, *N,N*-dimethyl-4-aminopyridine (DMAP), room temp, 41%; (d) NH_4OAc, $NaIO_4$, acetone, H_2O, room temp, 19−82%.

Scheme 4[a]

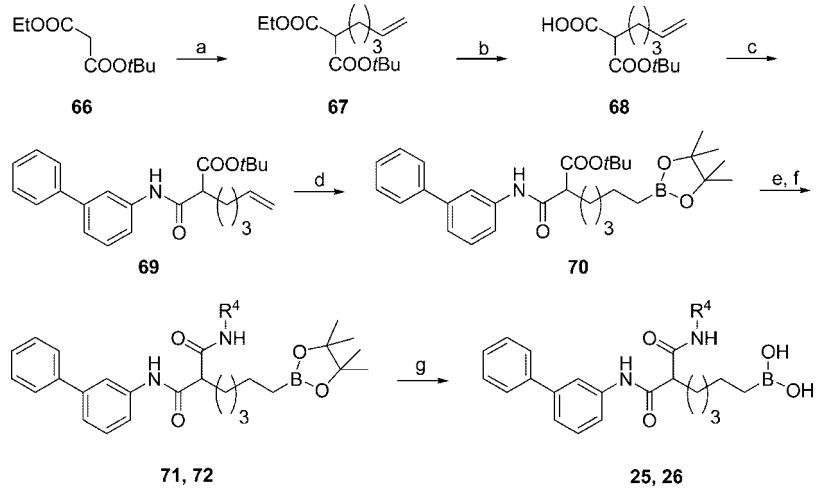

66 **67** **68** **69** **70** **71, 72** **25, 26**

71, **25** : R^4 = -Ph
72, **26** : R^4 = 3-pyridinyl

[a] Reagents and conditions: (a) NaH, 5-bromopent-1-ene, THF, reflux, 52%; (b) LiOH·H_2O, *tert*-BuOH, H_2O, 0 °C, 100%; (c) biphenyl-3-ylamine, EDCI, HOBt, DMF, room temp, 76%; (d) $[Ir(cod)Cl]_2$, dppm, pinacolborane, CH_2Cl_2, room temp, 70%; (e) TFA, room temp, 100%; (f) (i) oxalyl dichloride, DMF, CH_2Cl_2, 0 °C; (ii) R^4-NH_2, Et_3N, CH_2Cl_2, 0 °C, 29% for **71**, 51% for **72**; (g) NH_4OAc, $NaIO_4$, acetone, H_2O, room temp, 39% for **26**, 71% for **25**.

acids **5**−**10**, in which R^1 is various aromatic groups and R^2 is −NHBoc, were initially tested with an in vitro assay using HeLa nuclear extract with high HDAC activity (Table 1 and Figure S1). Compounds **5**−**10** showed HDAC-inhibitory activity at a concentration of 100 μM, while the 3-biphenyl **6**, 3-quinolinyl **7**, and benzthiazole **8** compounds were more potent (78−86% inhibition at 100 μM). Compounds **6**, **7**, and **8** inhibited HDAC activity dose-dependently with IC_{50} values of 12, 16, and 23 μM, respectively; these values are much lower than those of the other aromatic analogues **5**, **9**, and **10**. We also tested compounds **11**−**16**, which lack the NH-Boc group of compounds **5**−**10**, and they were found to be much less potent inhibitors than compounds **5**−**10** (Table 1 and Figure S1), suggesting the significance of the α-amino acid moiety.

To find more potent HDAC inhibitors, we next focused on the *tert*-butoxy group of compound **6**, the most potent inhibitor

Scheme 5[a]

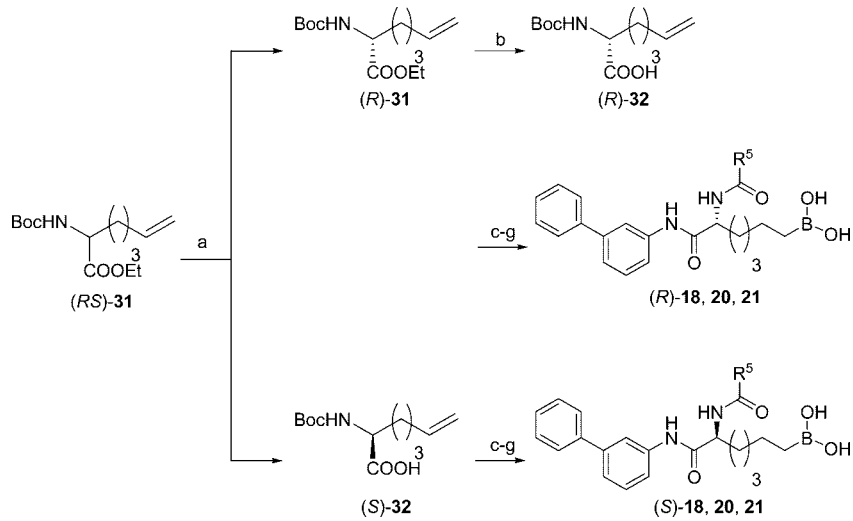

[a] Reagents and conditions: (a) subtilisin, H_2O/DMF (1:3), 37 °C, 42% for (*R*)-**31**, 50% for (*S*)-**32**; (b) LiOH·H_2O, EtOH, H_2O, room temp, 100%; (c) biphenyl-3-ylamine, EDCI, HOBt, DMF, room temp, 56−65%; (d) $[Ir(cod)Cl]_2$, dppm, pinacolborane, CH_2Cl_2, room temp, 79−82%; (e) HCl, AcOEt, $CHCl_3$, room temp, 100%; (f) R^5-COOH, EDCI, HOBt, DMF, room temp, 64−90%; (g) NH_4OAc, $NaIO_4$, acetone, H_2O, room temp, 4−87%.

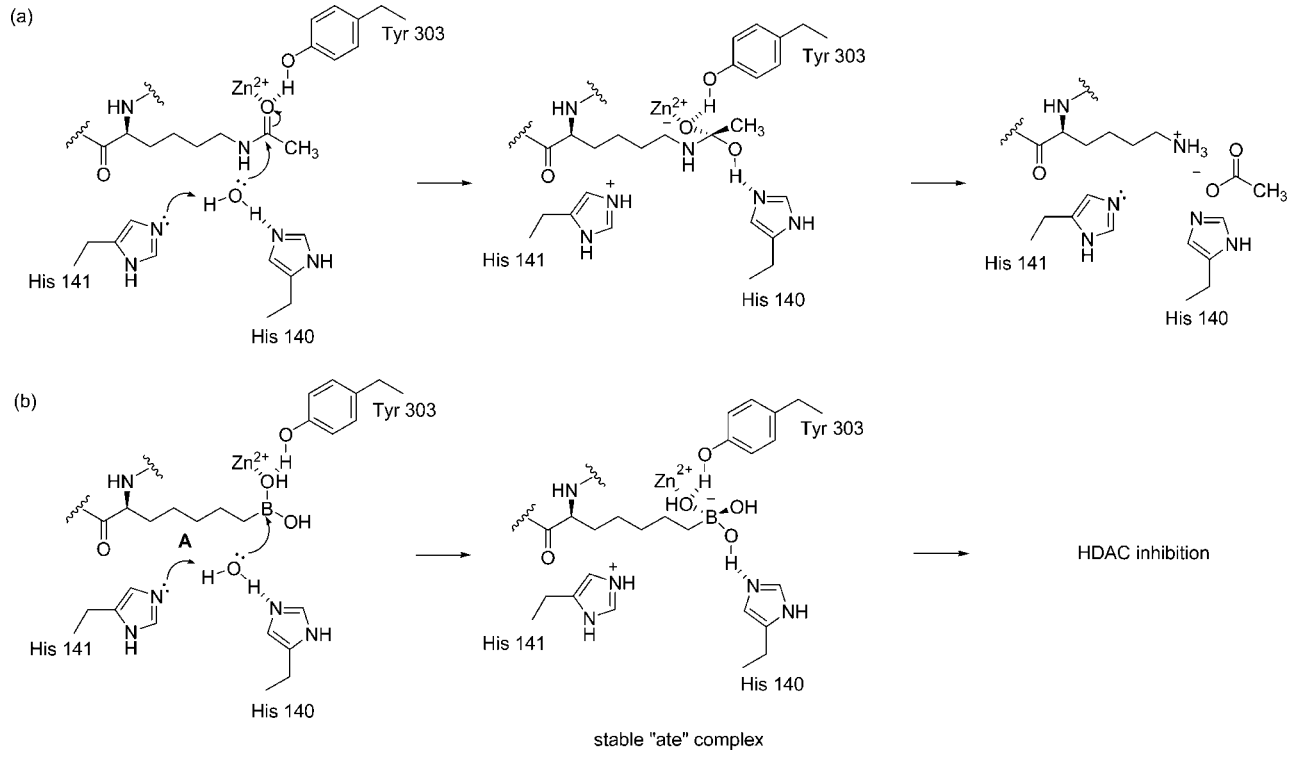

Figure 1. (a) Proposed mechanism for the deacetylation of acetylated lysine substrates. (b) Proposed mechanism of inhibition of HDACs by boronic acids **A**.

in Table 1. We initially changed the Boc group of compound **6** to a Cbz group (compound **17**) (Table 2 and Supporting Information Figure S2). Compound **17** exhibited about 3-fold higher potency than compound **6**. We also examined the activity of compound **18**, in which the benzyloxy group of compound **17** was replaced with a simple benzene ring, and the activity of **18** (IC_{50} = 2.0 μM) was about 2-fold higher than that of compound **17**. By the mimicking of the partial structure of TSA (**1**), we introduced the dimethylamino group at the 4-position of the phenyl ring of compound **18**, but compound **19** displayed a 6.5-fold decrease in potency compared to the parent compound **18**. Next, we converted the phenyl ring of compound **18** to various heteroaryl rings. The 2-indole **23** and 2-quinoline **24** compounds exhibited HDAC-inhibitory activity less potent than that of the phenyl compound **18**, whereas the 3-pyridine **20**, 5-thiazole **21**, and 4-thiazole **22** derivatives showed potencies similar to or greater than that of the phenyl compound **18** (IC_{50} values: **20** = 2.0 μM, **21** = 1.4 μM, **22** = 4.7 μM), highlighting the importance of small ring size.

To confirm the importance of α-amino acid structure, we examined the activity of malonic acid derivatives **25** and **26** in which the α-aminocarbonyl moiety of compounds **18** and **20** is replaced by the corresponding carboxamide (Table 2 and Figure S2). Compounds **25** and **26** showed about 15- and 25-fold decreases in potency compared with the parent compounds **18** and **20**, respectively.

Table 1. HDAC Inhibitory Activity of Boronic Acids **5**−**16**[a]

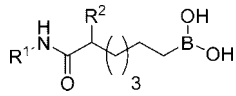

compd	R^1	R^2	% Inhbtn at 100 μM	IC_{50} (μM)
5	-Ph	-NHCOO*t*-Bu	42	>100
6		-NHCOO*t*-Bu	85	12
7		-NHCOO*t*-Bu	86	16
8		-NHCOO*t*-Bu	78	23
9		-NHCOO*t*-Bu	38	>100
10	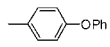	-NHCOO*t*-Bu	15	>100
11	-Ph	-H	37	>100
12		-H	40	>100
13		-H	32	>100
14		-H	5.1	>100
15		-H	1.8	>100
16	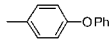	-H	2.2	>100

[a] Values are the mean of at least three experiments. IC_{50} of SAHA (**2**) is 0.28 μM.

Next we examined the influence of optical activity. Compounds (*R*)-**18**, **20**, **21** and (*S*)-**18**, **20**, **21** were prepared and evaluated for their inhibitory effects on HDAC1, HDAC2, HDAC6, and HDAC8, as well as total HDACs from nuclear extracts. As shown in Table 3 and Supporting Information Figure S3, in all cases, (*S*)-**18**, **20**, and **21** were at least 10-fold more active than (*R*)-**18**, **20**, and **21**, respectively. Since the stereochemistry of (*S*)-**18**, **20**, and **21** is the same as that of natural lysine, these results suggest that these boronic acids act in the active site of HDACs. Among (*S*)-**18**, **20**, and **21**, (*S*)-**21** was found to be the most potent inhibitor. Compound (*S*)-**21** inhibited all HDACs with IC_{50} values in the micromolar or submicromolar range. Although (*S*)-**21** was less potent than SAHA (**2**), the isoform inhibition profile of (*S*)-**21** was similar to that of **2**, which is the only HDAC inhibitor currently used in clinical practice.

Cellular Assays. To examine the effectiveness of boronic acid-based HDAC inhibitors as anticancer drugs and tools for biological research, compounds (*S*)-**18**, **20**, and **21**, as well as SAHA (**2**), were tested in a cancer cell growth inhibition assay. For initial screening, we used stomach cancer MKN45 cells because HDAC inhibitors have been reported to inhibit the cell growth of MKN45 cells.[20] The results are summarized in Table 4.

Table 2. HDAC Inhibitory Activity of **17**−**26**[a]

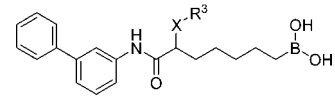

compd	R3	X	IC_{50} (μM)
6	-O*t*Bu	-NHCO-	12
17	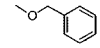	-NHCO-	4.2
18	-Ph	-NHCO-	2.0
19	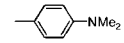	-NHCO-	13
20		-NHCO-	2.0
21		-NHCO-	1.4
22		-NHCO-	4.7
23	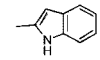	-NHCO-	11
24	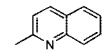	-NHCO-	>100
25	-Ph	-CONH-	30
26		-CONH-	51

[a] Values are the mean of at least three experiments.

Table 3. HDAC Inhibitory Activity of (*S*)- and (*R*)-**18**, **20**, **21**[a]

compd	IC_{50} (μM) HDAC (nuclear extract)	class I HDAC1	class I HDAC2	class I HDAC8	class II, HDAC6
2	0.28	0.35	0.25	1.7	0.028
(*S*)-**18**	1.6	>10[b]	3.6	>100	1.1
(*R*)-**18**	17	>100	>100	>100	24
(*S*)-**20**	1.4	2.8	0.83	23	0.32
(*R*)-**20**	15	>100	99	>100	14
(*S*)-**21**	0.92	2.2	0.53	6.6	0.11
(*R*)-**21**	24	>100	>100	>100	5.6

[a] Values are the mean of at least three experiments. [b] 38% inhibition at 10 μM.

Table 4. Growth-Inhibitory Activity on MKN45 Cells and GI_{50}/IC_{50} Values of SAHA (**2**) and (*S*)-**18**, **20**, **21**[a]

compd	GI_{50} (μM)	GI_{50}/IC_{50} HDAC	HDAC1	HDAC2
2	7.3	26	21	29
(*S*)-**18**	9.3	5.8	<0.93	2.6
(*S*)-**20**	5.5	3.9	2.0	6.6
(*S*)-**21**	3.5	3.8	1.6	6.6

[a] Values are the mean of two separate experiments.

SAHA (**2**) and its derivatives have been reported to show potent HDAC-inhibitory activity in enzyme assays and cancer cell growth inhibition assays.[21] However, a relatively large shift in potency between enzyme assay and cellular assay (GI_{50}/IC_{50}, abbreviated as potency shift in this paper) was observed with those hydroxamate HDAC inhibitors.[21] Indeed, as shown in Table 4, SAHA (**2**) exhibited a large potency shift in the cancer

Table 5. Growth Inhibition of Various Cancer Cells Using SAHA (**2**) and (*S*)-**21**[a]

		GI_{50} (μM)	
	cell	**2**	(*S*)-**21**
HBC-5	breast cancer	17	6.5
SNB-78	central nervous system	16	9.1
HCT116	colon cancer	0.58	0.73
DMS114	lung cancer	2.9	2.4
LOX-IMVI	melanoma	1.3	1.3
SK-OV-3	ovarian cancer	2.5	2.2
RXF-631 L	renal cancer	2.0	3.2
MKN45	stomach cancer	7.3	3.5
PC-3	prostate cancer	4.6	6.7
	mean	6.0	4.0

[a] Values are the mean of two separate experiments.

cell growth inhibition assay using MKN45 cells.[22] The reason for the large potency shift of SAHA (**2**) is unclear, but it seems reasonable to assume that it is at least partly due to poor membrane permeability resulting from the highly polar character of hydroxamic acid. Using Advanced Chemistry Development (ACD/Laboratories) software, version 8.14 for Solaris, the log *D* (pH 7) values of methylhydroxamic acid ($CH_3CONHOH$) and methylboronic acid ($CH_3B(OH)_2$) were calculated to be −1.59 and 1.0, respectively. The calculation results suggest that boronic acid is more lipophilic than hydroxamic acid under physiological conditions, and boronic acid derivatives might permeate through the cell membrane more efficiently than hydroxamates; therefore, they might not show such large potency shifts as hydroxamates like SAHA (**2**). We then evaluated the growth-inhibitory activity of (*S*)-**18**, **20**, and **21** on MKN45 cells. As we expected, (*S*)-**18**, **20**, and **21** inhibited the growth of MKN45 cells and showed smaller potency shift values than SAHA (**2**). Among (*S*)-**18**, **20**, and **21**, compound (*S*)-**21** showed the highest activity, being more potent than SAHA (**2**). Next, we evaluated growth inhibition by SAHA (**2**) and compound (*S*)-**21** against nine human cancer cell lines (Table 5). Compound (*S*)-**21** exerted potent growth inhibition against various human cancer cells, with GI_{50} values ranging from 0.73 to 9.1 μM, and these inhibitory activities were similar to those of SAHA (**2**) (average GI_{50} of (*S*)-**21** is 4.0 μM, that of SAHA is 6.0 μM). In addition, compound (*R*)-**21** did not show strong activity against these cancer cell lines (Table S1 and Figure S4 in Supporting Information) with GI_{50}s values ranging from 13 to 21 μM, suggesting the responsibility of HDAC inhibition for cancer cell growth repression.

Next, we performed Western blot analysis to examine the HDAC-inhibitory effects of boronic acid derivatives in cells. Since nuclear HDACs such as HDAC 1 and HDAC2 catalyze the deacetylation of histones,[3d] the acetylation level of histone H4 in human colon cancer HCT116 cells was analyzed after treatment of the cells with compounds (*S*)-**18**, **20**, and **21**. As can be seen in Figure 2, the level of acetylated histone H4 was elevated dose-dependently. The level of acetylated α-tubulin was also investigated because (*S*)-**18**, **20**, and **21** displayed potent inhibition of HDAC6, which is reported to catalyze the deacetylation of α-tubulin.[23] As expected, compounds (*S*)-**18**, **20**, and **21** caused a dose-dependent increase in acetylation of α-tubulin. These results suggest that the cancer cell growth inhibition by boronic acids (*S*)-**18**, **20**, and **21** was the result of HDAC inhibition.

Molecular Modeling. Since the results of the enzyme assays (Table 3) suggested that boronic acids act within the active center of HDACs, we studied the binding mode of hydrated (*S*)-**21** within this site. We calculated the low energy conformation of the hydrated (*S*)-**21** complex docked in a model based on the crystal structure of HDAC8 (PDB code 1T67) using Macromodel 9.6 software (Figure 3). An inspection of the complex shows that one of the oxygen atoms of the hydrated boronic acid can coordinate to the zinc ion (distance between oxygen and zinc, 2.04 Å) (Figure 3, left). In addition, the hydrogen of the OH group of Tyr 306 is located 1.95 and 2.20 Å from the two oxygen atoms of the hydrated boronic acid,

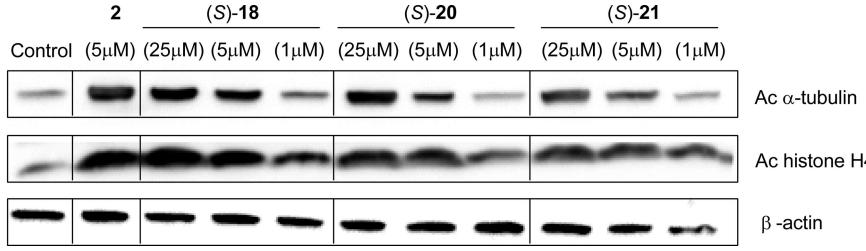

Figure 2. Western blot detection of acetylated α-tubulin and histone H4 levels in HCT116 cells after 8 h treatment with (*S*)-**18**, **20**, **21** and reference compound **2**.

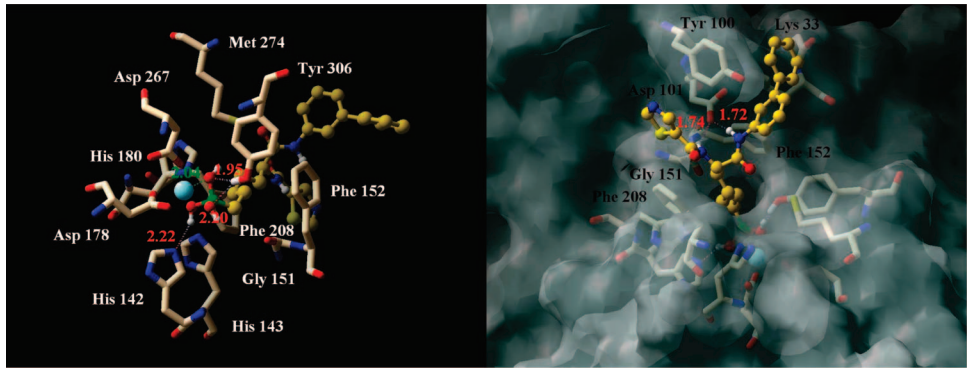

Figure 3. View of the conformation of (*S*)-**21** (ball-and-stick) docked in the HDAC8 catalytic core. Residues within 5 Å from the zinc ion are displayed in the tube graphic (left), and the surface of the enzyme is displayed in gray (right).

which suggests that Tyr 306 can form two hydrogen bonds with the hydrated boronic acid. Moreover, a short distance (2.22 Å) between one of the hydrogens of the hydrated boronic acid and the nitrogen of His 142 was also observed. This indicates that hydrated boronic acids inhibit HDACs by interacting with the zinc ion, Tyr residue, and His residue in the active center. On the surface of HDAC8, the biphenyl ring is located in the hydrophobic region formed by the benzene rings of Tyr 100 and Phe 152 and the alkyl chain of Lys 33, and the thiazole ring lies in the hydrophobic area formed by the benzene ring of Tyr100 and the methylene groups of Asp 101, Gly 151, and Phe 208 (Figure 3, right). It is also suggested that two hydrogen bonds can be formed between the two NH groups and the carboxylate anion of Asp 101 (the distances are 1.72 and 1.74 Å). The observed interactions between (*S*)-**21** and HDAC8 on the surface of the enzyme suggest the importance of the amino acid structure and the (*S*)-configuration of the inhibitor.

Conclusion

On the basis of the proposed catalytic mechanism for the deacetylation of acetylated lysine substrates by HDACs, we designed a series of boronic acids bearing an α-amino acid moiety as candidate mechanism-based HDAC inhibitors. Among the synthesized compounds, compounds (*S*)-**18**, **20**, and **21** displayed potent HDAC-inhibitory activities, suggesting that these boronic acids act in the active site of HDACs. Compounds (*S*)-**18**, **20**, and **21** also showed cancer cell growth-inhibitory activities as potent as SAHA (**2**). Intracellular HDAC inhibition by compounds (*S*)-**18**, **20**, and **21** was confirmed by Western blot analysis of acetylated histone H4 and acetylated α-tubulin. A molecular modeling study of the HDAC8/(*S*)-**21** complex suggested that the hydrated boronic acid interacts with zinc ion, Tyr residue, and His residue in the active site of HDACs.

Thus, we have identified a novel lead structure from which it should be possible to develop more potent HDAC inhibitors. Although boronic acids have been used as inhibitors for various hydrolytic enzymes such as serine protease,[24] arginase,[25] and proteasome,[26] this is the first report of HDAC inhibitors containing a boronic acid moiety. The results obtained in this study suggest that boronic acid-based inhibitors of HDACs have considerable potential for the development of novel therapeutic agents and tools for biological research.

Experimental Section

Chemistry. Melting points were determined using a Yanagimoto micro melting point apparatus or a Büchi 545 melting point apparatus and were left uncorrected. Proton nuclear magnetic resonance spectra (^{1}H NMR) and carbon nuclear magnetic resonance spectra (^{13}C NMR) were recorded with a JEOL JNM-LA500, JEOL JNM-A500, or Bruker Avance 600 spectrometer in solvents as indicated. Chemical shifts (δ) are reported in parts per million relative to the internal standard tetramethylsilane. Elemental analysis was performed with a Yanaco CHN CORDER NT-5 analyzer, and all values were within ±0.4% of the calculated values, which indicates >95% purity of the tested compounds. Fast atom bombardment (FAB) mass spectra were recorded on a JEOL JMS-SX102A mass spectrometer. In positive-mode MS analysis using 3-nitrobenzyl alcohol (NBA) as a matrix, boronic acids are esterified with NBA and the molecular weight detected corresponds to $(M + 2NBA - 2H_2O + H)^+$ or $(M + 2NBA - 2H_2O)^+$. In negative-mode analysis using glycerol (Gly) as a matrix, the molecular weight detected corresponds to $(M + Gly - 2H_2O - H)^-$. HPLC was performed with a Shimazu instrument equipped with a CHIRALPAK IA column (4.6 mm × 250 mm, Daicel Chemical Industries), and the samples eluted at 1 mL/min with ethanol and *n*-hexane. Reagents and solvents were purchased from Aldrich, Tokyo Kasei Kogyo, Wako Pure Chemical Industries, and Kanto Kagaku and used without purification. Flash column chromatography was performed using silica gel 60 (particle size 0.046−0.063 mm) supplied by Merck.

6-*tert*-Butoxycarbonylamino-7-oxo-7-phenylaminoheptylboronic Acid (5). Step 1: Preparation of Diethyl 2-*tert*-Butoxycarbonylaminomalonate (28). To a suspension of diethyl aminomalonate (**27**; 10.0 g, 47.2 mmol) and Et_3N (32.9 mL, 236 mmol) in THF (20 mL) was added a solution of $(Boc)_2O$ (20.6 g, 94.4 mmol) in THF (10 mL), and the solution was stirred overnight at room temperature. The reaction mixture was poured into water and extracted with AcOEt. The AcOEt layer was washed with water and brine and dried over Na_2SO_4. Filtration and concentration in vacuo and purification by silica gel flash column chromatography (AcOEt/*n*-hexane = 1/5) gave 10.5 g (81%) of **28** as a colorless oil: ^{1}H NMR ($CDCl_3$, 500 MHz, δ, ppm) 5.56 (1H, d, J = 6.7 Hz), 4.95 (1H, d, J = 7.6 Hz), 4.27 (4H, m), 1.45 (9H, s), 1.30 (6H, t, J = 7.3 Hz).

Step 2: Preparation of Diethyl 2-*tert*-Butoxycarbonylamino-2-(penten-4-yl)malonate (29). To a solution of **28** (10.2 g, 37.2 mmol) obtained above in EtOH (15 mL) was added NaOEt (2.78 g, 40.9 mmol) under Ar gas at 0 °C. The reaction mixture was stirred at 0 °C for 7 min. After that, to the solution was added 5-bromopent-1-ene (8.32 g, 55.8 mmol), and the mixture was refluxed for 10 h. It was then poured into water and extracted with AcOEt. The AcOEt layer was washed with water and brine and dried over Na_2SO_4. Filtration and concentration in vacuo and purification by silica gel flash column chromatography (AcOEt/*n*-hexane = 1/6) gave 11.3 g (89%) of **29** as a colorless oil: ^{1}H NMR ($CDCl_3$, 500 MHz, δ, ppm) 5.94 (1H, broad s), 5.76 (1H, ddt, J = 17, 10, 6.4 Hz), 5.00 (1H, dd, J = 15, 1.8 Hz), 4.95 (1H, d, J = 10 Hz), 4.26−4.18 (4H, m), 2.28 (2H, m), 2.07 (2H, q, J = 7.3 Hz), 1.43 (9H, s), 1.30−1.19 (8H, m).

Step 3: Preparation of 2-*tert*-Butoxycarbonylamino-2-(ethoxycarbonyl)hept-6-enoic Acid (30). To a solution of **29** (11.3 g, 33.0 mmol) obtained above in EtOH/H_2O (20 mL/10 mL) was added $LiOH\cdot H_2O$ (1.52 g, 36.3 mmol), and the solution was stirred overnight at 0 °C. The reaction mixture was neutralized with 10% citric acid and extracted with AcOEt. The AcOEt layer was washed with brine and dried over Na_2SO_4. Filtration and concentration in vacuo gave 10.3 g (99%) of **30** as a yellow oil: ^{1}H NMR ($CDCl_3$, 500 MHz, δ, ppm) 5.80−5.71 (2H, m), 5.01 (1H, dd, J = 17, 1.5 Hz), 4.97 (1H, dd, J = 10, 1.8 Hz), 4.31−4.18 (2H, m), 2.22 (2H, m), 2.07 (2H, m), 1.44 (9H, s), 1.39−1.22 (5H, m).

Step 4: Preparation of Ethyl 2-*tert*-Butoxycarbonylaminohept-6-enoate (31). A solution of **30** (10.3 g, 32.6 mmol) obtained above in toluene (40 mL) was refluxed for 9 h. The reaction mixture was concentrated and purified by flash column chromatography (AcOEt/*n*-hexane = 1/6) to give 8.51 g (94%) of **31** as a yellow oil: ^{1}H NMR ($CDCl_3$, 500 MHz, δ, ppm) 5.77 (1H, ddt, J = 17, 10, 6.7 Hz), 5.04−4.94 (3H, m), 4.28 (1H, m), 4.19 (2H, m), 2.07 (2H, m), 1.81 (1H, m,), 1.63 (1H, m), 1.53−1.37 (11H, m), 1.28 (3H, t, J = 7.3 Hz).

Step 5: Preparation of 2-*tert*-Butoxycarbonylaminohept-6-enoic Acid (32). To a solution of **31** (8.34 g, 30.8 mmol) obtained above in EtOH/H_2O (20 mL/10 mL) was added $LiOH\cdot H_2O$ (1.25 g, 29.8 mmol), and the solution was stirred overnight at 0 °C. The reaction mixture was neutralized with 10% citric acid and extracted with AcOEt. The AcOEt layer was washed with brine and dried over Na_2SO_4. Filtration and concentration in vacuo gave 7.01 g (94%) of **32** as a white solid: ^{1}H NMR ($CDCl_3$, 500 MHz, δ, ppm) 5.78 (1H, ddt, J = 17, 10, 6.7 Hz), 5.06−4.94 (3H, m), 4.32 (1H, m), 2.09 (2H, m), 1.87 (1H, m), 1.68 (1H, m), 1.57−1.37 (11H, m).

Step 6: Preparation of *tert*-Butyl 1-(Phenylaminocarbonyl) hex-5-en-1-ylcarbamate (33). To a solution of **32** (1.00 g, 4.11 mmol) and aniline (560 μL, 6.17 mmol) in DMF (15 mL) were added 1-ethyl-3-(3-dimethylaminopropyl)carbodiimide hydrochloride (EDCI; 1.18 g, 6.17 mmol) and 1-hydroxy-1*H*-benzotriazole monohydrate ($HOBt\cdot H_2O$; 834 mg, 6.17 mmol), and the mixture was stirred overnight at room temperature. The reaction mixture

was poured into water and extracted with AcOEt. The AcOEt layer was washed with water and brine and dried over Na_2SO_4. Filtration and concentration in vacuo and purification by silica gel flash column chromatography (AcOEt/*n*-hexane = 1/7) gave 875 mg (67%) of **33** as a white solid: ^{1}H NMR ($CDCl_3$, 500 MHz, δ, ppm) 8.26 (1H, broad s), 7.51 (2H, d, J = 7.6 Hz), 7.31 (2H, t, J = 7.6 Hz), 7.10 (1H, t, J = 7.3 Hz), 5.77 (1H, ddt, J = 17, 10, 6.7 Hz), 5.08 (1H, broad s), 5.01 (1H, dd, J = 17, 1.8 Hz), 4.96 (1H, d, J = 10 Hz), 4.20 (1H, m), 2.10 (2H, m), 1.95 (1H, m), 1.64 (1H, m), 1.57−1.40 (11H, m).

Step 7: Preparation of *tert*-Butyl 1-(Phenylaminocarbonyl)-6-(4,4,5,5,-tetramethyl-1,3,2-dioxaborolan-2-yl)hexylcarbamate (39). A solution of $[Ir(cod)Cl]_2$ (88.7 mg, 0.132 mmol) and bis(diphenylphosphino)methane (dppm; 100 mg, 0.264 mmol) in CH_2Cl_2 (10 mL) was stirred at room temperature for 5 min under Ar gas. After that, to the solution was added pinacolborane (300 μL, 2.00 mmol) and **33** (420 mg, 1.32 mmol) obtained above in CH_2Cl_2 (10 mL) in that order, and the mixture was stirred at room temperature for 2 days. The reaction mixture was concentrated and purified by silica gel flash column chromatography (AcOEt/*n*-hexane = 1/5) to give 397 mg (67%) of **39** as a white solid: ^{1}H NMR ($CDCl_3$, 500 MHz, δ, ppm) 8.15 (1H, broad s), 7.51 (2H, d, J = 7.6 Hz), 7.32 (2H, t, J = 7.9 Hz), 7.10 (1H, t, J = 7.6 Hz), 4.98 (1H, broad s), 4.13 (1H, m), 1.92 (1H, m), 1.64 (1H, m), 1.50−1.30 (15H, m), 1.24 (12H, s), 0.77 (2H, t, J = 7.3 Hz).

Step 8: Preparation of 6-*tert*-Butoxycarbonylamino-7-oxo-7-phenylaminoheptylboronic Acid (5). To a solution of **39** (213 mg, 0.478 mmol) in acetone/H_2O (6 mL/3 mL) were added $NaIO_4$ (307 mg, 1.43 mmol) and NH_4OAc (110 mg, 1.43 mmol), and the suspension was stirred at room temperature for 2 days. The reaction mixture was poured into water and extracted with AcOEt. The AcOEt layer was washed with water and brine and dried over Na_2SO_4. Filtration and concentration in vacuo and purification by silica gel flash column chromatography (AcOEt/*n*-hexane = 1/1) gave 161 mg (92%) of **5** as a white solid. The solid was recrystallized from AcOEt to give 20.5 mg of **5** as colorless crystals: mp 114−117 °C; ^{1}H NMR (DMSO-d_6, 500 MHz, δ, ppm) 9.92 (1H, s), 7.59 (2H, d, J = 7.6 Hz) 7.34 (2H, s), 7.30 (2H, t, J = 7.6 Hz), 7.04 (1H, t, J = 7.3 Hz), 6.98 (1H, d, J = 7.6 Hz), 4.02 (1H, m), 1.66−1.50 (2H, m), 1.38−1.16 (15H, m), 0.55 (2H, t, J = 7.6 Hz); ^{13}C NMR (DMSO-d_6, 500 MHz, δ, ppm) 171.43, 155.43, 139.00, 128.66, 123.14, 119.15, 77.95, 55.15, 32.37, 31.97, 31.85, 28.18, 25.55, 24.14; MS (FAB) m/z 635 (M + 2NBA − 2H_2O + H)$^+$, 419 (M + Gly − 2H_2O − H)$^-$. Anal. ($C_{18}H_{29}BN_2O_5$) C, H, N.

Compounds **6**−**10** were prepared from **32** and an appropriate amine using the procedure described for **5**. For the synthesis of **41** and **42**, dppe was used instead of dppm (step 7).

7-(Biphenyl-3-ylamino)-6-*tert*-butoxycarbonylamino-7-oxoheptylboronic Acid (6). Yield 41% (three steps) (223 mg); colorless crystals; mp 140−143 °C; ^{1}H NMR (DMSO-d_6, 500 MHz, δ, ppm) 10.03 (1H, s), 7.91 (1H, s), 7.61 (3H, m), 7.48 (2H, t, J = 7.9 Hz), 7.41−7.33 (5H, m), 7.00 (1H, d, J = 7.0 Hz), 4.05 (1H, q, J = 7.2 Hz), 1.70−1.50 (2H, m), 1.44−1.18 (15H, m), 0.56 (2H, t, J = 7.3 Hz); ^{13}C NMR (DMSO-d_6, 500 MHz, δ, ppm) 171.85, 155.67, 140.93, 140.24, 139.65, 129.54, 129.14, 127.75, 126.75, 121.85, 118.45, 117.67, 78.30, 60.81, 55.41, 32.46, 32.10, 31.97, 28.34, 25.68, 25.34, 2.28; MS (FAB) m/z 711 (M + 2NBA − 2H_2O)$^+$, 495 (M + Gly − 2H_2O − H)$^-$. Anal. ($C_{24}H_{33}BN_2O_5$) C, H, N.

6-*tert*-Butoxycarbonylamino-7-oxo-7-(quinolin-3-ylamino)heptylboronic Acid (7). Yield 31% (three steps) (632 mg); colorless crystals; mp 125−127 °C; ^{1}H NMR (DMSO-d_6, 500 MHz, δ, ppm) 10.45 (1H, s), 8.93 (1H, s), 8.71 (1H, s), 7.96 (1H, d, J = 8.5 Hz), 7.93 (1H, d, J = 7.9 Hz), 7.65 (1H, t, J = 7.3 Hz), 7.58 (1H, t, J = 7.0 Hz), 7.36 (2H, s), 7.12 (1H, d, J = 7.6 Hz), 4.11 (1H, m), 1.75−1.53 (2H, m), 1.48−1.19 (15H, m), 0.57 (2H, t, J = 7.6 Hz); ^{13}C NMR (DMSO-d_6, 500 MHz, δ, ppm) 172.35, 155.46, 144.43, 144.06, 132.60, 128.40, 127.75, 127.70, 127.57, 127.00, 122.11, 78.03, 55.17, 31.75, 31.71, 28.12, 25.51, 24.06; MS (FAB) m/z 686 (M + 2NBA − 2H_2O + H)$^+$, 470 (M + Gly − 2H_2O − H)$^-$. Anal. ($C_{21}H_{30}BN_3O_5 \cdot {}^1/_2H_2O$) C, H, N.

7-(Benzothiazol-2-ylamino)-6-*tert*-butoxycarbonylamino-7-oxoheptylboronic Acid (8). Yield 27% (three steps) (615 mg); colorless crystals; mp 128−130 °C; ^{1}H NMR (DMSO-d_6, 500 MHz, δ, ppm) 12.42 (1H, s), 7.98 (1H, d, J = 7.9 Hz), 7.75 (1H, d, J = 7.9 Hz), 7.44 (1H, t, J = 7.6 Hz), 7.36 (2H, s), 7.31 (1H, t, J = 7.6 Hz), 7.22 (1H, d, J = 7.3 Hz), 4.21 (1H, q, J = 7.0 Hz), 1.71−1.54 (2H, m), 1.46−1.16 (15H, m), 0.56 (2H, t, J = 7.6 Hz); ^{13}C NMR (DMSO-d_6, 500 MHz, δ, ppm) 172.76, 157.84, 155.56, 148.56, 131.46, 126.14, 123.57, 121.72, 120.53, 78.28, 54.59, 31.72, 31.39, 28.20, 27.89, 25.50, 24.10; MS (FAB) m/z 692 (M + 2NBA − 2H_2O + H)$^+$, 476 (M + Gly − 2H_2O − H)$^-$. Anal. ($C_{19}H_{28}BN_3O_5S \cdot {}^1/_2H_2O$) C, H, N.

6-*tert*-Butoxycarbonylamino-7-oxo-7-(3-phenoxyphenylamino)heptylboronic Acid (9). Yield 15% (three steps) (142 mg); colorless crystals; mp 89−91 °C; ^{1}H NMR (DMSO-d_6, 500 MHz, δ, ppm) 10.00 (1H, s), 7.40 (2H, t, J = 7.6 Hz), 7.36−7.26 (5H, m), 7.15 (1H, t, J = 7.3 Hz), 7.03 (2H, d, J = 7.9 Hz), 6.97 (1H, d, J = 7.6 Hz), 6.70 (1H, d, J = 7.9 Hz), 3.98 (1H, m), 1.62−1.46 (2H, m), 1.44−1.14 (15H, m), 0.55 (2H, t, J = 7.6 Hz); ^{13}C NMR (DMSO-d_6, 500 MHz, δ, ppm) 171.65, 157.07, 156.35, 155.45, 140.55, 130.04, 123.59, 118.92, 113.92, 113.14, 108.90, 77.98, 55.19, 31.83, 28.18, 25.57, 24.14; MS (FAB) m/z 727 (M + 2NBA − 2H_2O + H)$^+$, 511 (M + Gly − 2H_2O − H)$^-$. Anal. ($C_{24}H_{33}BN_2O_6$) C, H, N.

6-*tert*-Butoxycarbonylamino-7-oxo-7-(4-phenoxyphenylamino)heptylboronic Acid (10). Yield 9% (three steps) (81 mg); colorless crystals; mp 94−96 °C; ^{1}H NMR (DMSO-d_6, 500 MHz, δ, ppm) 9.96 (1H, s), 7.61 (2H, d, J = 8.8 Hz), 7.39−7.30 (4H, m), 7.10 (1H, t, J = 7.3 Hz), 7.03−6.90 (5H, m), 4.02 (1H, q, J = 6.9 Hz), 1.68−1.50 (2H, m), 1.46−1.14 (15H, m), 0.56 (2H, t, J = 7.6 Hz); ^{13}C NMR (DMSO-d_6, 500 MHz, δ, ppm) 171.32, 157.44, 155.47, 151.63, 134.98, 129.95, 122.92, 120.87, 119.53, 117.78, 78.00, 55.15, 31.99, 31.88, 28.22, 28.04, 25.58, 24.18; MS (FAB) m/z 726 (M + 2NBA − 2H_2O)$^+$, 511 (M + Gly − 2H_2O − H)$^-$. Anal. ($C_{24}H_{33}BN_2O_6$) C, H, N.

Compounds **11**−**16** were prepared from hept-6-enoic acid (**45**) and an appropriate amine using the procedure described for **5** (steps 6−8). For the synthesis of **54** and **55**, dppe was used instead of dppm (step 7).

7-Oxo-7-phenylaminoheptylboronic Acid (11). Yield 42% (three steps) (178 mg); colorless crystals; mp 100−102 °C; ^{1}H NMR (DMSO-d_6, 500 MHz, δ, ppm) 9.84 (1H, s), 7.58 (2H, d, J = 7.6 Hz), 7.36 (2H, s), 7.28 (2H, t, J = 7.6 Hz), 7.01 (1H, t, J = 7.3 Hz), 2.28 (2H, t, J = 7.6 Hz), 1.57 (2H, quintet, J = 7.6 Hz), 1.35−1.20 (6H, m), 0.57 (2H, t, J = 7.6 Hz); ^{13}C NMR (DMSO-d_6, 500 MHz, δ, ppm) 171.32, 139.33, 128.62, 122.90, 119.03, 36.49, 31.90, 28.64, 25.16, 24.11; MS (FAB) m/z 520 (M + 2NBA − 2H_2O + H)$^+$, 304 (M + Gly − 2H_2O − H)$^-$. Anal. ($C_{13}H_{20}BNO_3$) C, H, N.

7-(Biphenyl-3-yl)amino-7-oxoheptylboronic Acid (12). Yield 28% (three steps) (184 mg); colorless crystals; mp 105−107 °C; ^{1}H NMR (DMSO-d_6, 500 MHz, δ, ppm) 9.94 (1H, s), 7.92 (1H, s), 7.60 (2H, d, J = 7.3 Hz), 7.57 (1H, d, J = 8.8 Hz), 7.47 (2H, t, J = 7.9 Hz), 7.39−7.30 (5H, m), 2.31 (2H, t, J = 7.6 Hz), 1.59 (2H, quintet, J = 7.0 Hz), 1.37−1.21 (6H, m), 0.58 (2H, t, J = 7.9 Hz); ^{13}C NMR (DMSO-d_6, 500 MHz, δ, ppm) 171.36, 140.59, 140.13, 139.82, 129.15, 128.84, 127.41, 126.50, 121.22, 117.96, 117.22, 36.45, 31.81, 28.56, 25.05, 24.02; MS (FAB) m/z 596 (M + 2NBA − 2H_2O + H)$^+$, 380 (M + Gly − 2H_2O − H)$^-$. Anal. ($C_{19}H_{24}BNO_3$) C, H, N.

7-Oxo-7-(quinolin-3-yl)aminoheptylboronic Acid (13). Yield 65% (three steps) (72 mg); colorless crystals; mp 146−148 °C; ^{1}H NMR (DMSO-d_6, 500 MHz, δ, ppm) 10.35 (1H, s), 8.89 (1H, d, J = 2.4 Hz), 8.71 (1H, d, J = 2.4 Hz), 7.94 (1H, d, J = 8.2 Hz), 7.90 (1H, d, J = 7.3 Hz), 7.63 (1H, t, J = 7.0 Hz), 7.56 (1H, t, J = 7.0 Hz), 7.35 (2H, s), 2.39 (2H, t, J = 7.6 Hz), 1.63 (2H, quintet, J = 7.3 Hz), 1.38−1.21 (6H, m), 0.58 (2H, t, J = 7.6 Hz); ^{13}C NMR (DMSO-d_6, 500 MHz, δ, ppm) 172.11, 144.38, 143.97, 132.88, 128.41, 127.78, 127.52, 126.90, 121.64, 119, 36.29, 31.79,

28.54, 24.95, 24.01; MS (FAB) *m/z* 571 (M + 2NBA − $2H_2O$ + $H)^+$, 355 (M + Gly − $2H_2O$ − $H)^-$. Anal. ($C_{16}H_{21}BN_2O_3 \cdot H_2O$) C, H, N.

7-(Benzothiazol-2-yl)amino-7-oxoheptylboronic Acid (14). Yield 7% (three steps) (28 mg); colorless crystals; mp 121−124 °C; ^{1}H NMR (DMSO-d_6, 500 MHz, δ, ppm) 12.29 (1H, s), 7.96 (1H, d, J = 7.6 Hz), 7.73 (1H, d, J = 7.6 Hz), 7.43(1H, t, J = 7.3 Hz), 7.35 (2H, s), 7.30 (1H, t, J = 7.9 Hz), 2.48 (2H, t, J = 7.6 Hz), 1.61 (2H, quintet, J = 7.3 Hz), 1.37−1.20 (6H, m), 0.57 (2H, t, J = 7.9 Hz); ^{13}C NMR (DMSO-d_6, 500 MHz, δ, ppm) 172.24, 157.80, 148.44, 131.32, 125.93, 123.31, 121.53, 120.33, 35.10, 31.69, 28.40, 24.48, 23.95; MS (FAB) *m/z* 577 (M + 2NBA − $2H_2O$ + $H)^+$, 361 (M + Gly − $2H_2O$ − $H)^-$. Anal. ($C_{14}H_{19}BN_2O_3S$) C, H, N.

7-Oxo-7-(3-phenoxyphenyl)aminoheptylboronic Acid (15). Yield 21% (three steps) (84 mg); colorless crystals; mp 85−87 °C; ^{1}H NMR (DMSO-d_6, 500 MHz, δ, ppm) 9.91 (1H, s), 7.39 (2H, t, J = 7.6 Hz), 7.36−7.26 (5H, m), 7.15 (1H, t, J = 7.3 Hz), 7.02 (2H, d, J = 8.5 Hz), 6.67 (1H, d, J = 7.6 Hz), 2.25 (2H, t, J = 7.3 Hz), 1.53 (2H, quintet, J = 7.6 Hz), 1.34−1.18 (6H, m), 0.56 (2H, t, J = 7.6 Hz); ^{13}C NMR (DMSO-d_6, 500 MHz, δ, ppm) 171.43, 156.96, 156.43, 140.85, 129.99, 129.93, 123.48, 118.80, 113.78, 112.91, 108.85, 36.47, 31.83, 28.59, 25.00, 24.06; MS (FAB) *m/z* 612 (M + 2NBA − $2H_2O$ + $H)^+$, 396 (M + Gly − $2H_2O$ − $H)^-$. Anal. ($C_{19}H_{24}BNO_4$) C, H, N.

7-Oxo-7-(4-phenoxyphenyl)aminoheptylboronic Acid (16). Yield 37% (three steps) (270 mg); colorless crystals; mp 132 °C; ^{1}H NMR (DMSO-d_6, 500 MHz, δ, ppm) 9.86 (1H, s), 7.60 (2H, d, J = 8.8 Hz), 7.36 (2H, t, J = 7.9 Hz), 7.33 (2H, s),7.09 (1H, d, J = 7.3 Hz), 6.99−6.92 (4H, m), 2.27 (2H, t, J = 7.6 Hz), 1.57 (2H, quintet, J = 7.3 Hz), 1.36−1.20 (6H, m), 0.57 (2H, t, J = 7.9 Hz); ^{13}C NMR (DMSO-d_6, 600 MHz, δ, ppm) 171.00, 157.36, 151.31, 135.25, 129.82, 122.78, 120.60, 119.35, 117.65, 79.06, 36.33, 31.80, 28,56, 25.11, 24.03; MS (FAB) *m/z* 612 (M + 2NBA − $2H_2O$ + $H)^+$, 396 (M + Gly − $2H_2O$ − $H)^-$. Anal. ($C_{19}H_{24}BNO_4$) C, H, N.

6-(Benzyloxycarbonylamino)-7-(biphenyl-3-ylamino)-7-oxoheptylboronic Acid (17). Steps 1 and 2: Preparation of Benzyl 1-(Biphenyl-3-ylaminocarbonyl)-6-(4,4,5,5,-tetramethyl-1,3,2-dioxaborolan-2-yl)hexylcarbamate (58). To a solution of **40** (600 mg, 1.15 mmol) in $CHCl_3$ (3 mL) was added 4 N HCl/AcOEt (3 mL), and the mixture was stirred at room temperature for 2 h. The reaction mixture was poured into 2 N aqueous NaOH and extracted with CH_2Cl_2. The CH_2Cl_2 layer was washed with brine and dried over Na_2SO_4. Filtration and concentration in vacuo gave 498 mg (100%) of 2-amino-*N*-(biphenyl-3-yl)-7-(4,4,5,5,-tetramethyl-1,3,2-dioxaborolan-2-yl)heptanamide as a yellow oil: ^{1}H NMR ($CDCl_3$, 500 MHz, δ, ppm) 9.57 (1H, s), 7.85 (1H, s), 7.63−7.58 (3H, m), 7.45−7.30 (5H, m), 3.49 (1H, m), 1.97 (1H, m), 1.63−1.30 (9H, m), 1.24 (12H, s), 0.78 (2H, t, J = 7.6 Hz).

To a solution of 2-amino-*N*-(biphenyl-3-yl)-7-(4,4,5,5,-tetramethyl-1,3,2-dioxaborolan-2-yl)heptanamide (250 mg, 0.592 mmol) obtained above and a catalytic amount of *N*,*N*-dimethyl-4-aminopyridine (DMAP) in CH_2Cl_2 (3 mL) were added benzyloxycarbonyl chloride (202 μL, 1.18 mmol) and Et_3N (0.5 mL, 3.58 mmol), and the mixture was stirred at room temperature for 3 h. The reaction mixture was poured into water and extracted with AcOEt. The AcOEt layer was washed with water and brine and dried over Na_2SO_4. Filtration and concentration in vacuo and purification by silica gel flash column chromatography (AcOEt/*n*-hexane = 1/3) gave 134 mg (41%) of **58** as a white solid: ^{1}H NMR ($CDCl_3$, 500 MHz, δ, ppm) 8.20 (1H, s), 7.76 (1H, s), 7.57 (2H, d, J = 7.3 Hz), 7.49 (1H, m), 7.42 (2H, t, J = 7.3 Hz), 7.38−7.24 (8H, m), 5.35 (1H, broad s), 5.13 (2H, s), 4.26 (1H, m), 1.94 (1H, m), 1.69 (1H, m), 1.45−1.15 (18H, m), 0.76 (2H, t, J = 7.0 Hz).

Step 3: Preparation of 6-(Benzyloxycarbonylamino)-7-(biphenyl-3-ylamino)-7-oxoheptylboronic Acid (17). Compound **17** was prepared from **58** using the procedure described for **5** (step 8) in 32% yield (84 mg): colorless crystals; mp 141−142 °C; ^{1}H NMR (DMSO-d_6, 500 MHz, δ, ppm) 10.12 (1H, s), 7.92 (1H, s), 7.64−7.55 (4H, m), 7.48 (2H, t, J = 7.3 Hz), 7.43−7.28 (10H, m), 5.04 (2H, d, J = 2.1 Hz), 4.13 (1H, q, J = 7.4 Hz), 1.72−1.54 (2H, m), 1.46−1.19 (6H, m), 0.56 (2H, t, J = 7.6 Hz); ^{13}C NMR (DMSO-d_6, 500 MHz, δ, ppm) 171.36, 156.09, 140.74, 140.12, 139.52, 137.01, 129.34, 128.95, 128.32, 127.77, 127.68, 127.56, 126.60, 121.66, 118.23, 117.49, 79.14, 65.39, 55.59, 31.90, 31.82, 25.57, 24.59, 24.15; MS (FAB) *m/z* 745 (M + 2NBA − $2H_2O$ + $H)^+$, 529 (M + Gly − $2H_2O$ − $H)^-$. Anal. ($C_{27}H_{31}BN_2O_5$) C, H, N.

6-(Benzenecarbonylamino)-7-(biphenyl-3-ylamino)-7-oxoheptylboronic Acid (18). Step 1: Preparation of 1-(Biphenyl-3-ylaminocarbamoyl)-6-(4,4,5,5,-tetramethyl-1,3,2-dioxaborolan-2-yl)hexylbenzamide (59). To a solution of 2-amino-*N*-(biphenyl-3-yl)-7-(4,4,5,5,-tetramethyl-1,3,2-dioxaborolan-2-yl)heptanamide (240 mg, 0.568 mmol) obtained above and benzoic acid (104 mg, 0.852 mmol) in DMF (10 mL) were added EDCI (163 mg, 0.852 mmol) and HOBt·H_2O (130 mg, 0.852 mmol), and the mixture was stirred overnight at room temperature. The reaction mixture was poured into water and extracted with AcOEt. The AcOEt layer was washed with water and brine and dried over Na_2SO_4. Filtration and concentration in vacuo and purification by silica gel flash column chromatography (AcOEt/*n*-hexane = 1/3) gave 192 mg (64%) of **59** as a white solid: ^{1}H NMR ($CDCl_3$, 500 MHz, δ, ppm) 8.73 (1H, s), 7.84−7.80 (3H, m), 7.59−7.51 (4H, m), 7.47−7.31 (7H, m), 6.81 (1H, d, J = 8.2 Hz), 4.83 (1H, q, J = 7.3 Hz), 2.08 (1H, m), 1.83 (1H, m), 1.51−1.31 (6H, m), 1.22 (12H, s), 0.76 (2H, t, J = 7.9 Hz).

Step 2: Preparation of 6-(Benzenecarbonylamino)-7-(biphenyl-3-ylamino)-7-oxoheptylboronic Acid (18). Compound **18** was prepared from **59** using the procedure described for **5** (step 8) in 79% yield (127 mg): colorless crystals; mp 112−113 °C; ^{1}H NMR (DMSO-d_6, 500 MHz, δ, ppm) 10.21 (1H, s), 8.59 (1H, d, J = 7.6 Hz), 7.95 (1H, s), 7.92 (2H, d, J = 7.0 Hz), 7.64−7.59 (3H, m), 7.55 (1H, t, J = 7.3 Hz), 7.48 (2H, t, J = 7.3 Hz), 7.47 (2H, t, J = 7.9 Hz), 7.43−7.32 (5H, m), 4.57 (1H, q, J = 7.4 Hz), 1.82 (2H, q, J = 7.6 Hz), 1.51−1.23 (6H, m), 0.57 (2H, t, J = 7.0 Hz); ^{13}C NMR (DMSO-d_6, 500 MHz, δ, ppm) 171.30, 166.60, 140.74, 140.13, 139.61, 134.03, 131.31, 129.33, 128.95, 128.17, 127.56, 121.63, 118.24, 117.50, 54.59, 31.64, 25.87, 24.18; MS (FAB) *m/z* 715 (M + 2NBA − $2H_2O$ + $H)^+$, 499 (M + Gly − $2H_2O$ − $H)^-$. Anal. ($C_{26}H_{29}BN_2O_4$) C, H, N.

Compounds **19**−**24** were prepared from 2-amino-*N*-(biphenyl-3-yl)-7-(4,4,5,5,-tetramethyl-1,3,2-dioxaborolan-2-yl)heptanamide and an appropriate carboxylic acid using the procedure described for **18**.

7-(Biphenyl-3-ylamino)-6-(*N*,*N*-dimethyl-4-aminobenzenecarbonylamino]-7-oxoheptylboronic Acid (19). Yield 11% (three steps) (51 mg); colorless crystals; mp 178−180 °C; ^{1}H NMR (DMSO-d_6, 500 MHz, δ, ppm) 10.15 (1H, s), 8.16 (1H, d, J = 7.9 Hz), 7.95 (1H, s), 7.80 (2H, d, J = 9.1 Hz), 7.64−7.58 (3H, m), 7.47 (2H, t, J = 7.9 Hz), 7.42−7.31 (5H, m), 6.71 (2H, d, J = 8.8 Hz), 4.53 (1H, q, J = 7.3 Hz), 2.98 (6H, s), 1.79 (2H, q, J = 7.0 Hz), 1.48−1.22 (6H, m), 0.57 (2H, t, J = 8.5 Hz); ^{13}C NMR (DMSO-d_6, 600 MHz, δ, ppm) 171.65, 166.31, 152.09, 140.64, 140.58, 139.57, 129.22, 128.85, 127.45, 126.51, 121.46, 120.50, 118.09, 117.35, 110.55, 54.31, 31.83, 31.64, 30.59, 25.78, 24.10; MS (FAB) *m/z* 757 (M + 2NBA − $2H_2O)^+$, 542 (M + Gly − $2H_2O$ − $H)^-$. Anal. ($C_{28}H_{34}BN_3O_4$) C, H, N.

7-(Biphenyl-3-ylamino)-7-oxo-6-(pyridine-3-carbonylamino)-heptylboronic Acid (20). Yield 62% (three steps) (162 mg); colorless crystals; mp 134−135 °C; ^{1}H NMR (DMSO-d_6, 500 MHz, δ, ppm) 10.24 (1H, s), 9.07 (1H, d, J = 1.5 Hz), 8.85 (1H, d, J = 7.6 Hz), 8.72 (1H, dd, J = 4.5, 1.8 Hz), 8.26 (1H, dt, J = 8.2, 1.8 Hz), 7.95 (1H, s), 7.64−7.57 (3H, m), 7.52 (1H, dd, J = 7.8, 4.9 Hz), 7.47 (2H, t, J = 7.9 Hz), 7.43−7.32 (5H, m), 4.58 (1H, q, J = 7.6 Hz), 1.82 (2H, m), 1.52−1.20 (6H, m), 0.57 (2H, t, J = 7.3 Hz); ^{13}C NMR (DMSO-d_6, 600 MHz, δ, ppm) 171.04, 165.26, 148.71, 140.77, 140.12, 139.56, 135.31, 129.55, 129.36, 128.97, 127.58, 126.62, 123.38, 118.31, 117.56, 54.61, 31.88, 31.62, 25.84, 24.17; MS (FAB) *m/z* 716 (M + 2NBA − $2H_2O$ + $H)^+$, 500 (M + Gly − $2H_2O$ − $H)^-$. Anal. ($C_{25}H_{28}BN_3O_4$) C, H, N.

7-(Biphenyl-3-ylamino)-7-oxo-6-(thiazole-5-carbonylamino)-heptylboronic Acid (21). Yield 54% (three steps) (201 mg); colorless crystals; mp 145−147 °C; ^{1}H NMR (DMSO-d_6, 500 MHz, δ, ppm) 10.24 (1H, s), 9.24 (1H, s), 8.89 (1H, d, J = 7.6 Hz), 8.66 (1H, s), 7.94 (1H, s), 7.64−7.57 (3H, m), 7.47 (2H, t, J = 7.9 Hz), 7.43−7.30 (5H, m), 4.56 (1H, q, J = 7.4 Hz), 1.81 (2H, m), 1.50−1.24 (6H, m), 0.57 (2H, t, J = 7.9 Hz); ^{13}C NMR (DMSO-d_6, 500 MHz, δ, ppm) 170.71, 159.97, 158.00, 144.01, 140.67, 140.01, 139.38, 135.06, 129.26, 128.85, 127.46, 121.66, 121.66, 118.20, 117.47, 54.37, 31.73, 31.57, 25.66, 24.04; MS (FAB) m/z 722 (M + 2NBA − 2H$_2$O + H)$^+$, 506 (M + Gly − 2H$_2$O − H)$^-$. Anal. ($C_{23}H_{26}BN_3O_4S\cdot{}^1/_2H_2O$) C, H, N.

7-(Biphenyl-3-ylamino)-7-oxo-6-(thiazole-4-carbonylamino)-heptylboronic Acid (22). Yield 31% (three steps) (207 mg); colorless crystals; mp 96−97 °C; ^{1}H NMR (DMSO-d_6, 500 MHz, δ, ppm) 10.28 (1H, s), 9.22 (1H, d, J = 2.1 Hz), 8.38 (1H, d, J = 1.8 Hz), 8.28 (1H, d, J = 8.2 Hz), 7.93 (1H, s), 7.63−7.57 (3H, m), 7.47 (2H, t, J = 7.9 Hz), 7.44−7.31 (5H, m), 4.66 (1H, q, J = 7.4 Hz), 1.83 (2H, m), 1.42−1.22 (6H, m), 0.55 (2H, t, J = 7.6 Hz); ^{13}C NMR (DMSO-d_6, 600 MHz, δ, ppm) 170.40, 160.02, 158.01, 150.05, 140.71, 139.95, 139.20, 129.31, 128.87, 127.50, 126.53, 124.52, 121.80, 118.24, 117.51, 53.37, 32.38, 31.74, 25.21, 24.04; MS (FAB) m/z 722 (M + 2NBA − 2H$_2$O + H)$^+$, 506 (M + Gly − 2H$_2$O − H)$^-$. Anal. ($C_{23}H_{26}BN_3O_4S$) C, H, N.

7-(Biphenyl-3-ylamino)-6-(1*H*-indole-2-carbonylamino)-7-oxoheptylboronic Acid (23). Yield 44% (three steps) (123 mg); colorless crystals; mp 141−142 °C; ^{1}H NMR (DMSO-d_6, 500 MHz, δ, ppm) 11.59 (1H, s), 10.26 (1H, s), 8.60 (1H, d, J = 7.3 Hz), 7.95 (1H, s), 7.68−7.58 (4H, m), 7.50−7.30 (9H, m), 7.19 (1H, t, J = 7.0 Hz), 7.04 (1H, t, J = 7.0 Hz), 4.62 (1H, q, J = 7.4 Hz), 1.82 (2H, m), 1.50−1.25 (6H, m), 0.57 (2H, t, J = 8.2 Hz); ^{13}C NMR (DMSO-d_6, 500 MHz, δ, ppm) 171.21, 161.19, 140.76, 140.12, 139.56, 136.47, 131.23, 129.35, 128.95, 127.56, 127.03, 126.61, 123.40, 121.69, 121.56, 119.71, 118.29, 117.55, 112.25, 103.61, 79.15, 54.09, 31.89, 31.82, 25.78, 24.19; MS (FAB) m/z 754 (M + 2NBA − 2H$_2$O + H)$^+$, 538 (M + Gly − 2H$_2$O − H)$^-$. Anal. ($C_{28}H_{30}BN_3O_4\cdot{}^1/_2H_2O$) C, H, N.

7-(Biphenyl-3-ylamino)-7-oxo-6-(quinoline-2-carbonylamino)-heptylboronic Acid (24). Yield 56% (three steps) (165 mg); colorless crystals; mp 127−128 °C; ^{1}H NMR (DMSO-d_6, 500 MHz, δ, ppm) 10.40 (1H, s), 8.88 (1H, d, J = 8.2 Hz), 8.61 (1H, d, J = 8.5 Hz), 8.22 (1H, d, J = 8.8 Hz), 8.19 (1H, d, J = 8.5 Hz), 8.11 (1H, d, J = 7.6 Hz), 7.97 (1H, s), 7.90 (1H, d, J = 7.3 Hz), 7.75 (1H, t, J = 7.9 Hz), 7.65−7.57 (3H, m), 7.50−7.32 (7H, m), 4.78 (1H, q, J = 7.4 Hz), 1.91 (2H, m), 1.45−1.26 (6H, m), 0.56 (2H, t, J = 7.3 Hz); ^{13}C NMR (DMSO-d_6, 500 MHz, δ, ppm) 170.43, 163.48, 149.42, 145.93, 140.82, 140.03, 139.26, 138.13, 130.69, 129.42, 129.29, 128.96, 128.25, 128.11, 127.60, 126.63, 121.96, 118.54, 118.39, 117.67, 53.62, 32.77, 31.87, 25.26, 24.12; MS (FAB) m/z 766 (M + 2NBA − 2H$_2$O + H)$^+$, 550 (M + Gly − 2H$_2$O − H)$^-$. Anal. ($C_{29}H_{30}BN_3O_4$) C, H, N.

7-(Biphenyl-3-ylamino)-7-oxo-6-(phenylaminocarbonyl)heptylboronic Acid (25). Step 1: Preparation of *tert*-Butyl Ethyl 2-(Pent-4-enyl)malonate (67). To a solution of *tert*-butyl ethyl malonate (**66**; 5.11 g, 27.1 mmol) in dry THF (30 mL) was added NaH (50%, 1.43 g, 29.9 mmol) under Ar gas at 0 °C. The reaction mixture was stirred at 0 °C for 5 min. After that, 5-bromopent-1-ene was added (4.45 g, 29.9 mmol), and the mixture was refluxed for 10 h. It was then poured into water and extracted with AcOEt. The AcOEt layer was washed with water and brine and dried over Na_2SO_4. Filtration and concentration in vacuo and purification by silica gel flash column chromatography (AcOEt/*n*-hexane = 1/100 to 1/50) gave 4.02 g (52%) of **67** as a colorless oil: ^{1}H NMR ($CDCl_3$, 500 MHz, δ, ppm) 5.79 (1H, ddt, J = 17, 10, 6.7 Hz), 5.02 (1H, dd, J = 17, 1.5 Hz), 4.96 (1H, d, J = 10 Hz), 4.19 (2H, m), 3.22 (1H, t, J = 7.6 Hz), 2.08 (2H, q, J = 7.0 Hz), 1.86 (2H, q, J = 7.6 Hz), 1.48−1.38 (11H, m), 1.27 (3H, t, J = 7.0 Hz).

Step 2: Preparation of 2-*tert*-Butoxycarbonylhept-6-enoic Acid (68). To a solution of **67** (2.00 g, 7.80 mmol) in *tert*-BuOH/H$_2$O (10 mL/5 mL) was added LiOH·H$_2$O (360 mg, 8.58 mmol), and the solution was stirred overnight at 0 °C. The reaction mixture was neutralized with 10% citric acid and extracted with AcOEt. The AcOEt layer was washed with brine and dried over Na_2SO_4. Filtration and concentration in vacuo gave 1.80 g (100%) of **68** as a yellow oil: ^{1}H NMR ($CDCl_3$, 500 MHz, δ, ppm) 5.78 (1H, ddt, J = 17, 10, 6.7 Hz), 5.03 (1H, dd, J = 17, 1.5 Hz), 4.98 (1H, d, J = 10 Hz), 3.29 (1H, t, J = 7.3 Hz), 2.09 (2H, q, J = 7.3 Hz), 1.91 (2H, m), 1.51−1.40 (11H, m).

Step 3: Preparation of *tert*-Butyl 2-(Biphenyl-3-ylaminocarbonyl)hept-6-enoate (69). Compound **69** was prepared from **68** using the procedure described for **5** (step 6) in 76% yield: a white solid; ^{1}H NMR ($CDCl_3$, 500 MHz, δ, ppm) 8.86 (1H, s), 7.78 (1H, s), 7.60 (2H, d, J = 7.3 Hz), 7.55 (1H, d, J = 7.6 Hz), 7.46−7.30 (5H, m), 5.78 (1H, ddt, J = 17, 10, 6.7 Hz), 5.02 (1H, dd, J = 17, 1.5 Hz), 4.98 (1H, d, J = 10 Hz), 3.27 (1H, t, J = 7.3 Hz), 2.11 (2H, q, J = 7.0 Hz), 1.99 (2H, m), 1.52−1.48 (11H, m).

Step 4: Preparation of *tert*-Butyl 2-(Biphenyl-3-ylaminocarbonyl)-7-(4,4,5,5-tetramethyl-1,3,2-dioxaborolan-2-yl)heptanoate (70). Compound **70** was prepared from **69** using the procedure described for **5** (step 7) in 70% yield: a white solid; ^{1}H NMR ($CDCl_3$, 500 MHz, δ, ppm) 8.86 (1H, s), 7.78 (1H, s), 7.60 (2H, d, J = 7.3 Hz), 7.56 (1H, d, J = 8.3 Hz), 7.46−7.31 (5H, m), 3.26 (1H, t, J = 7.6 Hz), 1.96 (2H, m), 1.50 (9H, s), 1.46−1.30 (6H, s), 1.23 (12H, s), 0.77 (2H, t, J = 7.9 Hz).

Steps 5 and 6: Preparation of *N*-Biphenyl-3-yl-*N*′-phenyl-2-[5-(4,4,5,5-tetramethyl-1,3,2-dioxaborolan-2-yl)]pentylmalonamide (71). A solution of **70** (637 mg, 1.26 mmol) in TFA (5 mL) was stirred at room temperature for 3 h. The reaction mixture was concentrated in vacuo to give 580 mg (100%) of 2-(biphenyl-3-ylaminocarbonyl)-7-(4,4,5,5-tetramethyl-1,3,2-dioxaborolan-2-yl) heptanoic acid as a yellow oil: ^{1}H NMR ($CDCl_3$, 500 MHz, δ, ppm) 8.31 (1H, s), 7.77 (1H, s), 7.59 (2H, d, J = 7.0 Hz), 7.51 (1H, d, J = 7.0 Hz), 7.47−7.34 (5H, m), 3.40 (1H, t, J = 7.3 Hz), 2.06 (2H, m), 1.52−1.30 (6H, m), 1.24 (12H, d, J = 1.8 Hz), 0.80 (2H, t, J = 7.6 Hz).

To a solution of 2-(biphenyl-3-ylaminocarbonyl)-7-(4,4,5,5-tetramethyl-1,3,2-dioxaborolan-2-yl)heptanoic acid (357 mg, 0.790 mmol) obtained above in CH_2Cl_2 (5 mL) were added ethanedioxalyl dichloride (151 μL, 1.19 mmol) and a catalytic amount of DMF, and the mixture was stirred at room temperature for 3 h. It was then concentrated in vacuo, and the residue was dissolved in CH_2Cl_2 (5 mL). To a solution of aniline (111 mg, 1.19 mmol) and Et_3N (2 mL, 14.3 mmol) in CH_2Cl_2 (5 mL) was added a solution of the acid chloride in CH_2Cl_2 (5 mL) at 0 °C, and the mixture was stirred at room temperature for 2 h. The reaction mixture was poured into water and extracted with CH_2Cl_2. The CH_2Cl_2 layer was washed with water and brine and dried over Na_2SO_4. Filtration and concentration in vacuo and purification by silica gel flash column chromatography (AcOEt/*n*-hexane = 1/5) gave 122 mg of **71** (29%) as a white solid: ^{1}H NMR ($CDCl_3$, 500 MHz, δ, ppm) 8.82 (1H, s), 8.67 (1H, s), 7.81 (1H, s), 7.62−7.54 (5H, m), 7.46−7.31 (7H, m), 7.14 (1H, t, J = 7.3 Hz), 3.31 (1H, t, J = 7.3 Hz), 2.09 (2H, q, J = 7.6 Hz), 1.52−1.34 (6H, m), 1.24 (12H, s), 0.77 (2H, t, J = 7.6 Hz).

Step 7: Preparation of 7-(Biphenyl-3-ylamino)-7-oxo-6-(phenylaminocarbonyl)heptylboronic Acid (25). Compound **25** was prepared from **71** using the procedure described for **5** (step 8) in 71% yield (73 mg): colorless crystals; mp 99−100 °C; ^{1}H NMR (DMSO-d_6, 500 MHz, δ, ppm) 10.03 (1H, s), 9.95 (1H, s), 7.94 (1H, s), 7.65−7.56 (5H, m), 7.52−7.26 (9H, m), 7.06 (1H, t, J = 6.7 Hz), 3.49 (1H, t, J = 8.4 Hz), 1.91 (2H, m), 1.45−1.22 (6H, m), 0.57 (2H, t, J = 7.6 Hz); ^{13}C NMR (DMSO-d_6, 500 MHz, δ, ppm) 168.08, 167.89, 140.76, 144.04, 139.42, 138.82, 129.36, 128.95, 128.71, 127.57, 126.60, 123.47, 121.84, 119.40, 118.37, 117.65, 55.21, 32.02, 29.74, 27.15, 24.10; MS (FAB) m/z 715 (M + 2NBA − 2H$_2$O + H)$^+$, 499 (M + Gly − 2H$_2$O − H)$^-$. Anal. ($C_{26}H_{29}BN_2O_4$) C, H, N.

Compound **26** was prepared from 2-(biphenyl-3-ylaminocarbonyl)-7-(4,4,5,5-tetramethyl-1,3,2-dioxaborolan-2-yl)heptanoic acid and a pyridin-3-ylamine using the procedure described for **25**.

7-(Biphenyl-3-ylamino)-7-oxo-6-(pyridin-3-ylaminocarbonyl) heptylboronic Acid (26). Yield 20% (two steps) (112 mg); colorless crystals; mp 128−129 °C; ^{1}H NMR (DMSO-d_6, 500 MHz, δ, ppm) 10.24 (1H, s), 10.15 (1H, s), 8.84 (1H, d, J = 2.1 Hz), 8.34 (1H, d, J = 4.3 Hz), 8.14 (1H, d, J = 8.5 Hz), 8.02 (1H, s), 7.71−7.66 (3H, m), 7.55 (2H, t, J = 7.6 Hz), 7.51−7.40 (6H, m), 3.61 (1H, t, J = 7.6 Hz), 2.00 (2H, m), 1.45−1.30 (6H, m), 0.65 (2H, t, J = 7.3 Hz); ^{13}C NMR (DMSO-d_6, 500 MHz, δ, ppm) 168.39, 167.78, 144.32, 144.01, 140.91, 140.67, 139.33, 135.44, 129.28, 128.87, 127.50, 126.33, 123.53, 121.78, 117.57, 55.05, 31.93, 29.53, 27.10, 24.01; MS (FAB) m/z 716 (M + 2NBA − 2H_2O + H)$^+$, 500 (M + Gly − 2H_2O − H)$^-$. Anal. ($C_{25}H_{28}BN_3O_4 \cdot {}^1/_2H_2O$) C, H, N.

(*R*)-6-(Benzenecarbonylamino)-7-(biphenyl-3-ylamino)-7-oxoheptylboronic Acid ((*R*)-18). Step 1: Preparation of (*S*)-2-*tert*-Butoxycarbonylaminohept-6-enoic Acid ((*S*)-32) and (*R*)-Ethyl 2-*tert*-Butoxycarbonylaminohept-6-enoate ((*R*)-31). Compound (*RS*)-**31** (10.8 g, 39.8 mmol) was suspended in a mixture of H_2O (750 mL) and DMF (150 mL) (1/3, v/v) solvent system at 37 °C, and the pH was adjusted to about 7−8 by adding 1 M aqueous ammonia solution. Then, subtilisin (39.8 mg, 1 mg of enzyme per mmol of substrate) was added and the pH was maintained at 7−8 by continuous addition of 1 M aqueous ammonia solution. The reaction was completed within 5 h. The solvents were evaporated, and the residue was poured into 2 N aqueous NaOH and extracted with diethyl ether. The diethyl ether layer was washed with water and brine and dried over Na_2SO_4. Filtration and concentration in vacuo gave 5.28 g (49%) of (*R*)-**31** as a yellow oil. Then, the aqueous solution was acidified and extracted with AcOEt. The AcOEt layer was washed with brine and dried over Na_2SO_4. Filtration and concentration in vacuo gave 5.92 g of (*S*)-**32** (50%) as a white solid: ^{1}H NMR ($CDCl_3$, 500 MHz, δ, ppm) 5.79 (1H, ddt, J = 17, 10, 6.7 Hz), 5.08−4.92 (3H, m), 4.32 (1H, m), 2.09 (2H, m), 1.87 (1H, m), 1.69 (1H, m), 1.56−1.35 (11H, m). Compound (*R*)-**31** (5.28 g, 19.5 mmol) was further resolved with 5.00 mg of subtilisin using the same procedure as described above to give pure (*R*)-**31** (4.52 g, 42%) as a yellow oil: ^{1}H NMR ($CDCl_3$, 500 MHz, δ, ppm) 5.77 (1H, ddt, J = 17, 10, 6.7 Hz), 5.03−4.95 (3H, m), 4.28 (1H, m), 4.23−4.15 (2H, m), 2.07 (2H, m), 1.81 (1H, m), 1.62 (1H, m), 1.53−1.35 (11H, m), 1.28 (3H, t, J = 7.3 Hz).

Step 2: Preparation of (*R*)-2-*tert*-Butoxycarbonylaminohept-6-enoic Acid ((*R*)-32). Compound (*R*)-**32** was prepared from (*R*)-**31** using the procedure described for **5** (step 5) in 100% yield: a white solid; ^{1}H NMR ($CDCl_3$, 500 MHz, δ, ppm) 5.78 (1H, ddt, J = 17, 10, 6.7 Hz), 5.06−4.94 (3H, m), 4.32 (1H, m), 2.09 (2H, m), 1.87 (1H, m), 1.69 (1H, m), 1.57−1.35 (11H, m).

Steps 3−7: Preparation of (*R*)-6-(Benzenecarbonylamino)-7-(biphenyl-3-ylamino)-7-oxoheptylboronic Acid ((*R*)-18). Compound (*R*)-**18** was prepared from (*R*)-**32** using the procedure described for **5** (steps 6 and 7) and **18** (steps 1 and 2) in 2% yield (>99% ee) (five steps) (21 mg). In this case, biphenyl-3-ylamine was used instead of aniline: colorless crystals; HPLC t_R = 7.98 min (ethanol/*n*-hexane = 7/93); mp 100−102 °C; ^{1}H NMR (DMSO-d_6, 500 MHz, δ, ppm) 10.21 (1H, s), 8.58 (1H, d, J = 7.6 Hz), 7.95 (1H, s), 7.93 (2H, d, J = 7.3 Hz), 7.65−7.58 (3H, m), 7.55 (1H, t, J = 7.3 Hz), 7.48 (2H, t, J = 7.6 Hz), 7.48 (2H, t, J = 7.3 Hz), 7.43−7.32 (5H, m), 4.57 (1H, q, J = 7.4 Hz), 1.82 (2H, q, J = 7.6 Hz), 1.51−1.24 (6H, m), 0.58 (2H, t, J = 7.9 Hz); ^{13}C NMR (DMSO-d_6, 600 MHz, δ, ppm) 171.39, 166.71, 140.82, 140.18, 139.65, 134.06, 131.40, 129.41, 129.02, 128.26, 127.61, 126.67, 121.72, 118.31, 117.56, 54.67, 31.95, 31.69, 25.93, 24.24; MS (FAB) m/z 715 (M + 2NBA − 2H_2O + H)$^+$, 499 (M + Gly − 2H_2O − H)$^-$. Anal. ($C_{26}H_{29}BN_2O_4 \cdot {}^1/_2H_2O$) C, H, N.

Compounds (*R*)-**20** and (*R*)-**21** were prepared from (*R*)-**32** and an appropriate amine using the procedure described for (*R*)-**18**.

(*R*)-7-(Biphenyl-3-ylamino)-7-oxo-6-(pyridine-3-carbonylamino)heptylboronic Acid ((*R*)-20). Yield 34% (>99% ee) (five steps) (463 mg); colorless crystals; HPLC t_R = 10.93 min (ethanol/*n*-hexane = 15/85); mp 142−143 °C; ^{1}H NMR (DMSO-d_6, 500 MHz, δ, ppm) 10.24 (1H, s), 9.07 (1H, d, J = 1.5 Hz), 8.84 (1H, d, J = 7.3 Hz), 8.73 (1H, dd, J = 4.5, 1.8 Hz), 8.26 (1H, d, J = 7.9 Hz), 7.95 (1H, s), 7.65−7.58 (3H, m), 7.53 (1H, dd, J = 7.6, 4.6 Hz), 7.48 (2H, t, J = 7.9 Hz), 7.44−7.33 (5H, m), 4.59 (1H, q, J = 7.3 Hz), 1.83 (2H, m), 1.52−1.25 (6H, m), 0.59 (2H, t, J = 7.0 Hz); ^{13}C NMR (DMSO-d_6, 500 MHz, δ, ppm) 171.06, 165.30, 151.98, 148.71, 140.80, 140.14, 139.56, 135.34, 129.60, 129.38, 128.99, 127.60, 126.63, 123.41, 121.76, 118.37, 117.62, 54.66, 31.88, 31.65, 25.85, 24.18; MS (FAB) m/z 716 (M + 2NBA − 2H_2O + H)$^+$, 500 (M + Gly − 2H_2O − H)$^-$. Anal. ($C_{25}H_{28}BN_3O_4 \cdot {}^1/_2H_2O$) C, H, N.

(*R*)-7-(Biphenyl-3-ylamino)-7-oxo-6-(thiazole-5-carbonylamino)heptylboronic Acid ((*R*)-21). Yield 25% (>99% ee) (five steps) (351 mg); colorless crystals; HPLC t_R = 13.25 min (ethanol/*n*-hexane = 10/90); mp 138−139 °C; ^{1}H NMR (DMSO-d_6, 500 MHz, δ, ppm) 10.33 (1H, s), 9.31 (1H, s), 8.97 (1H, d, J = 7.3 Hz), 8.73 (1H, s), 8.01 (1H, s), 7.71−7.65 (3H, m), 7.54 (2H, t, J = 7.6 Hz), 7.51−7.40 (5H, m), 4.63 (1H, q, J = 7.3 Hz), 1.88 (2H, m), 1.57−1.32 (6H, m), 0.65 (2H, t, J = 7.6 Hz); ^{13}C NMR (DMSO-d_6, 600 MHz, δ, ppm) 170.91, 160.17, 158.20, 144.16, 140.84, 140.15, 139.52, 135.21, 129.45, 129.04, 127.65, 126.67, 121.85, 118.37, 117.62, 54.56, 31.89, 31.70, 25.82, 24.20; MS (FAB) m/z 722 (M + 2NBA − 2H_2O + H)$^+$, 506 (M + Gly − 2H_2O − H)$^-$. Anal. ($C_{23}H_{26}BN_3O_4S \cdot {}^1/_2H_2O$) C, H, N.

(*S*)-6-(Benzenecarbonylamino)-7-(biphenyl-3-ylamino)-7-oxoheptylboronic Acid ((*S*)-18). Compound (*S*)-**18** was prepared from (*S*)-**32** using the procedure described for **5** (steps 6 and 7), and **18** (steps 1 and 2) in 23% yield (99% ee) (five steps) (647 mg). In this case, biphenyl-3-ylamine was used instead of aniline: colorless crystals; HPLC t_R = 10.97 min (ethanol/*n*-hexane = 7/93); mp 102−104 °C; ^{1}H NMR (DMSO-d_6, 500 MHz, δ, ppm) 10.28 (1H, s), 8.64 (1H, d, J = 7.6 Hz), 8.01 (1H, s), 7.99 (2H, d, J = 7.6 Hz), 7.71−7.65 (3H, m), 7.62 (1H, t, J = 7.6 Hz), 7.55 (2H, t, J = 7.6 Hz), 7.54 (2H, t, J = 7.6 Hz), 7.50−7.39 (5H, m), 4.63 (1H, q, J = 7.3 Hz), 1.89 (2H, q, J = 7.6 Hz), 1.58−1.30 (6H, m), 0.65 (2H, t, J = 7.9 Hz); ^{13}C NMR (DMSO-d_6, 500 MHz, δ, ppm) 171.42, 166.81, 140.86, 140.20, 139.64, 134.09, 131.45, 129.46, 129.06, 128.1731, 127.67, 127.63, 126.69, 121.79, 118.39, 117.64, 54.72, 36.24, 31.96, 31.27, 25.93, 24.26; MS (FAB) m/z 715 (M + 2NBA − 2H_2O + H)$^+$, 499 (M + Gly − 2H_2O − H)$^-$. Anal. ($C_{26}H_{29}BN_2O_4 \cdot {}^1/_2H_2O$) C, H, N.

(*S*)-7-(Biphenyl-3-ylamino)-7-oxo-6-(pyridine-3-carbonylamino)heptylboronic Acid ((*S*)-20). Yield 32% (95% ee) (five steps) (533 mg); colorless crystals; HPLC t_R = 14.47 min (ethanol/*n*-hexane = 15/85); mp 138−140 °C; ^{1}H NMR (DMSO-d_6, 500 MHz, δ, ppm) 10.24 (1H, s), 9.07 (1H, d, J = 1.5 Hz), 8.85 (1H, d, J = 7.3 Hz), 8.73 (1H, dd, J = 4.5, 1.8 Hz), 8.26 (1H, d, J = 8.2 Hz), 7.95 (1H, s), 7.65−7.58 (3H, m), 7.53 (1H, dd, J = 7.6, 4.9 Hz), 7.48 (2H, t, J = 7.9 Hz), 7.44−7.33 (5H, m), 4.58 (1H, q, J = 7.5 Hz), 1.83 (2H, m), 1.52−1.25 (6H, m), 0.58 (2H, t, J = 7.0 Hz); ^{13}C NMR (DMSO-d_6, 500 MHz, δ, ppm) 171.09, 165.34, 152.00, 148.71, 140.82, 140.16, 139.56, 135.37, 129.62, 129.41, 129.02, 127.63, 126.66, 123.45, 121.80, 118.40, 117.65, 54.68, 31.90, 31.66, 25.85, 24.20; MS (FAB) m/z 716 (M + 2NBA − 2H_2O + H)$^+$, 500 (M + Gly − 2H_2O − H)$^-$. Anal. ($C_{25}H_{28}BN_3O_4 \cdot {}^1/_2H_2O$) C, H, N.

(*S*)-7-(Biphenyl-3-ylamino)-7-oxo-6-(thiazole-5-carbonylamino)heptylboronic Acid ((*S*)-21). Yield 26% (>99% ee) (five steps) (435 mg); colorless crystals; HPLC t_R = 17.72 min (ethanol/*n*-hexane = 10/90); mp 140−142 °C; ^{1}H NMR (DMSO-d_6, 500 MHz, δ, ppm) 10.27 (1H, s), 9.24 (1H, s), 8.92 (1H, d, J = 7.3 Hz), 8.67 (1H, s), 7.95 (1H, s), 7.67−7.56 (3H, m), 7.48 (2H, t, J = 7.6 Hz), 7.45−7.30 (5H, m), 4.56 (1H, q, J = 7.3 Hz), 1.82 (2H, m), 1.53−1.22 (6H, m), 0.59 (2H, t, J = 7.3 Hz); ^{13}C NMR (DMSO-d_6, 600 MHz, δ, ppm) 170.94, 160.20, 158.22, 144.18, 140.86, 140.16, 139.54, 135.23, 129.47, 129.06, 127.67, 126.69, 121.87, 118.40, 117.65, 54.59, 31.90, 31.72, 25.84, 24.22; MS (FAB) m/z 722 (M + 2NBA − 2H_2O + H)$^+$, 506 (M + Gly − 2H_2O − H)$^-$. Anal. ($C_{23}H_{26}BN_3O_4S \cdot {}^1/_2H_2O$) C, H, N.

Biology. Enzyme Assays. Assays of total HDAC activity and HDAC1, 2, 6, and 8 activities were performed using SIRT1 fluorescence activity assay/drug discovery kits (AK-500 and AK-555) with HeLa nuclear extract total (HDACs) or human recom-

binant HDAC1, 2, 6, and 8 (SE-456, SE-500, SE-508, and SE-145, respectively) produced by BIOMOL Research Laboratories, according to the supplier's instructions. The fluorescence of the wells was measured on a fluorometric reader with excitation set at 360 nm and emission detection set at 460 nm, and the % inhibition was calculated from the fluorescence readings of inhibited wells relative to those of control wells. The concentration of test compound that results in 50% inhibition was determined by plotting log [Inh] versus the logit function of the % inhibition. IC_{50} values were determined using regression analysis of the concentration/inhibition data.

Cell Growth Inhibition Assay. The details of cell growth inhibition measurement are described elsewhere.[27] Briefly, the cells were plated at appropriate density in 96-well plates in RPMI 1640 with 5% fetal bovine serum and allowed to attach overnight. The cells were exposed to drugs for 48 h. Then, the cell growth was determined by means of sulforhodamine B assay, as described by Skehan et al.[28] Calculations were made according to the method described previously.[27a] Absorbance values of control wells (C) and test wells (T) were measured at 525 nm. Moreover, absorbance of the test wells (T_0) was also measured at time 0 (addition of drugs). By use of these measurements, cell growth inhibition (percentage of growth) by a test drug at each concentration used was calculated as % growth $= 100 \times [(T - T_0)/(C - T_0)]$, when $T > T_0$, and % growth $= 100 \times [(T - T_0)/T]$, when $T < T_0$. By use of the computer to process % growth values, the 50% growth inhibition parameter (GI_{50}) was determined. The GI_{50} was calculated as $100 \times [(T - T_0)/(C - T_0)] = 50$.

Western Blot Analysis. Human colon cancer HCT116 cells were purchased from American Type Culture Collection (ATCC, Manassas, VA) and cultured in McCoy5A culture medium containing penicillin and streptomycin, which was supplemented with fetal bovine serum as described in the ATCC instructions. HCT-116 cells (5×10^5) were treated for 8 h with samples at the indicated concentrations in 10% FBS supplemented with McCoy's 5A medium and were then collected and extracted with SDS buffer. Protein concentrations of the lysates were determined using a Bradford protein assay kit (Bio-Rad Laboratories) with which equivalent amounts of protein from each lysate were resolved in 15% SDS−polyacrylamide gels. Bands were transferred onto nitrocellulose membranes (Bio-Rad Laboratories). The transblotted membranes were blocked for 30 min with Tris-buffered saline (TBS) containing 3% skimmed milk, then incubated overnight at 4 °C with hyperacetylated histone H4 antibody (Upstate Biotechnology) (1:4000 dilution), acetylated α-tubulin antibody (SIGMA) (1:2000 dilution), or β-actin antibody (Abcam) (1:500 dilution) in TBS containing 3% skimmed milk. After the membrane had been probed with the primary antibody, it was washed twice with water, then incubated with goat antirabbit or antimouse IgG-horseradish peroxidase conjugates (diluted 1:5000) for 2 h at room temperature and washed twice more with water. The immunoblots were visualized by enhanced chemiluminescence.

Molecular Modeling. Docking and subsequent scoring were performed using Macromodel 9.6 software. Coordinates of HDAC8 complxed with MS344 were taken from the Brookhaven Protein Data Bank (PDB code 1T67), and hydrogen atoms were added computationally at appropriate positions. The structure of compound (*S*)-**21** bound to HDAC8 was constructed by molecular mechanics (MM) energy minimization. The starting position of compound (*S*)-**21** was determined manually: the biphenyl ring and the linker parts were superimposed on the active site of the crystallographic MS344 counterpart. The conformation of compound (*S*)-**21** in the active site was minimized by MM calculation based on the OPLS_2005 force field with parameters set as follows: method, LBFGS; maximum number of iterations, 10 000; converge on, gradient; convergence threshold, 0.05.

Acknowledgment. This work was supported in part by a Grant-in-Aid for Scientific Research from the Japan Society for the Promotion of Science (N.M.).

Supporting Information Available: Results of elemental analysis of **5**−**26**, (*S*)-**18**, **20**, **21**, and (*R*)-**18**, **20**, **21**; Figures S1−S4 showing in vitro activities and cell growth inhibition; Table S1 listing growth inhibition results. This material is available free of charge via the Internet at http://pubs.acs.org.

References

(1) (a) Sterner, D. E.; Berger, S. L. Acetylation of histones and transcription-related factors. *Microbiol. Mol. Biol. Rev.* **2000**, *64*, 435–459. (b) Yoshida, M.; Shimazu, T.; Matsuyama, A. Protein deacetylases: enzymes with functional diversity as novel therapeutic targets. *Prog. Cell Cycle Res.* **2003**, *5*, 269–278. (c) Konstantinopoulos, P. A.; Karamouzis, M. V.; Papavassiliou, A. G. Focus on acetylation: the role of histone deacetylase inhibitors in cancer therapy and beyond. *Expert Opin. Invest. Drugs* **2007**, *16*, 569–571.

(2) (a) Biel, M.; Wascholowski, V.; Giannis, A. Epigenetics. An epicenter of gene regulation: histones and histone-modifying enzymes. *Angew. Chem., Int. Ed.* **2005**, *44*, 3186–3216. (b) Mai, A.; Massa, S.; Rotili, D.; Cerbara, I.; Valente, S.; Pezzi, R.; Simeoni, S.; Ragno, R. Histone deacetylation in epigenetics: an attractive target for anticancer therapy. *Med. Res. Rev.* **2005**, *25*, 261–309. (c) Suzuki, T.; Miyata, N. Epigenetic control using natural products and synthetic molecules. *Curr. Med. Chem.* **2006**, *13*, 935–958. (d) Schäfer, S.; Jung, M. Chromatin modifications as targets for new anticancer drugs. *Arch. Pharm.* **2005**, *338*, 347–357. (e) Itoh, Y.; Suzuki, T.; Miyata, N. Isoform-selective histone deacetylase inhibitors. *Curr. Pharm. Des.* **2008**, *14*, 529–544.

(3) (a) Grozinger, C. M.; Schreiber, S. L. Deacetylase enzymes: biological functions and the use of small-molecule inhibitors. *Chem. Biol.* **2002**, *9*, 3–16. (b) Kouzarides, T. Acetylation: a regulatory modification to rival phosphorylation. *EMBO J.* **2000**, *19*, 1176–1179. (c) Kouzarides, T. Histone acetylases and deacetylases in cell proliferation. *Curr. Opin. Genet. Dev.* **1999**, *9*, 40–48. (d) Hassig, C. A.; Schreiber, S. L. Nuclear histone acetylases and deacetylases and transcriptional regulation: HATs off to HDACs. *Curr. Opin. Chem. Biol.* **1997**, *1*, 300–308.

(4) (a) Sambucetti, L. C.; Fischer, D. D.; Zabludoff, S.; Kwon, P. O.; Chamberlin, H.; Trogani, N.; Xu, H.; Cohen, D. Histone deacetylase inhibition selectively alters the activity and expression of cell cycle proteins leading to specific chromatin acetylation and antiproliferative effects. *J. Biol. Chem.* **1999**, *274*, 34940–34947. (b) Hirose, T.; Sowa, Y.; Takahashi, S.; Saito, S.; Yasuda, C.; Shindo, N.; Furuichi, K.; Sakai, T. p53-independent induction of Gadd45 by histone deacetylase inhibitor: coordinate regulation by transcription factors Oct-1 and NF-Y. *Oncogene* **2003**, *22*, 7762–7773. (c) Klisovic, D. D.; Katz, S. E.; Effron, D.; Klisovic, M. I.; Wickham, J.; Parthun, M. R.; Guimond, M.; Marcucci, G. Depsipeptide (FR901228) inhibits proliferation and induces apoptosis in primary and metastatic human uveal melanoma cell lines. *Invest. Ophthalmol. Visual Sci.* **2003**, *44*, 2390–2398.

(5) (a) Yoshida, M.; Kijima, M.; Akita, M.; Beppu, T. Potent and specific inhibition of mammalian histone deacetylase both in vivo and in vitro by trichostatin A. *J. Biol. Chem.* **1990**, *265*, 17174–17179. (b) Yoshida, M.; Horinouchi, S.; Beppu, T. Trichostatin A and trapoxin: novel chemical probes for the role of histone acetylation in chromatin structure and function. *BioEssays* **1995**, *17*, 423–430.

(6) (a) Richon, V. M.; Emiliani, S.; Verdin, E.; Webb, Y.; Breslow, R.; Rifkind, R. A.; Marks, P. A. A class of hybrid polar inducers of transformed cell differentiation inhibits histone deacetylases. *Proc. Natl. Acad. Sci. U.S.A.* **1998**, *95*, 3003–3007. (b) Richon, V. M.; Webb, Y.; Merger, R.; Sheppard, T.; Jursic, B.; Ngo, L.; Civoli, F.; Breslow, R.; Rifkind, R. A.; Marks, P. A. Second generation hybrid polar compounds are potent inducers of transformed cell differentiation. *Proc. Natl. Acad. Sci. U.S.A.* **1996**, *93*, 5705–5708.

(7) Plumb, J. A.; Finn, P. W.; Williams, R. J.; Bandara, M. J.; Romero, M. R.; Watkins, C. J.; La Thangue, N. B.; Brown, R. Pharmacodynamic response and inhibition of growth of human tumor xenografts by the novel histone deacetylase inhibitor PXD101. *Mol. Cancer Ther.* **2003**, *2*, 721–728.

(8) Suzuki, T.; Ando, T.; Tsuchiya, K.; Fukazawa, N.; Saito, A.; Mariko, Y.; Yamashita, T.; Nakanishi, O. Synthesis and histone deacetylase inhibitory activity of new benzamide derivatives. *J. Med. Chem.* **1999**, *42*, 3001–3003.

(9) (a) Leoni, F.; Zaliani, A.; Bertolini, G.; Porro, G.; Pagani, P.; Pozzi, P.; Donà, G.; Fossati, G.; Sozzani, S.; Azam, T.; Bufler, P.; Fantuzzi, G.; Goncharov, I.; Kim, S.-H.; Pomerantz, B. J.; Reznikov, L. L.; Siegmund, B.; Dinarello, C. A.; Mascagni, P. The antitumor histone deacetylase inhibitor suberoylanilide hydroxamic acid exhibits anti-inflammatory properties via suppression of cytokines. *Proc. Natl. Acad. Sci. U.S.A.* **2002**, *99*, 2995–3000. (b) Dompierre, J. P.; Godin, J. D.; Charrin, B. C.; Cordelières, F. P.; King, S. J.; Humbert, S.; Saudou, F. Histone deacetylase 6 inhibition compensates for the transport deficit in Huntington's disease by increasing tubulin acetylation. *J. Neurosci.* **2007**, *27*, 3571–3583.

(10) Huangfu, D.; Maehr, R.; Guo, W.; Eijkelenboom, A.; Snitow, M.; Chen, A. E.; Melton, D. A. Induction of pluripotent stem cells by defined factors is greatly improved by small-molecule compounds. *Nat. Biotechnol.* **2008**, *26*, 795–797.

(11) (a) Suzuki, T.; Nagano, Y.; Kouketsu, A.; Matsuura, A.; Maruyama, S.; Kurotaki, M.; Nakagawa, H.; Miyata, N. Novel inhibitors of human histone deacetylases: design, synthesis, enzyme inhibition, and cancer cell growth inhibition of SAHA-based non-hydroxamates. *J. Med. Chem.* **2005**, *48*, 1019–1032. (b) Suzuki, T.; Kouketsu, A.; Itoh, Y.; Hisakawa, S.; Maeda, S.; Yoshida, M.; Nakagawa, H.; Miyata, N. Highly potent and selective histone deacetylase 6 inhibitors designed based on a small-molecular substrate. *J. Med. Chem.* **2006**, *49*, 4809–4812. (c) Itoh, Y.; Suzuki, T.; Kouketsu, A.; Suzuki, N.; Maeda, S.; Yoshida, M.; Nakagawa, H.; Miyata, N. Design, synthesis, structure−selectivity relationship, and effect on human cancer cells of a novel series of histone deacetylase 6-selective inhibitors. *J. Med. Chem.* **2007**, *50*, 5425–5438. (d) Miller, T. A.; Witter, D. J.; Belvedere, S. Histone deacetylase inhibitors. *J. Med. Chem.* **2003**, *46*, 5097–5116. (e) Paris, M.; Porcelloni, M.; Binaschi, M.; Fattori, D. Histone deacetylase inhibitors: from bench to clinic. *J. Med. Chem.* **2008**, *51*, 1505–1529.

(12) Jones, P.; Bottomley, M. J.; Casfí, A.; Cecchetti, O.; Ferrigno, F.; Lo Surdo, P.; Ontoria, J. M.; Rowley, M.; Scarpelli, R.; Schultz-Fademrecht, C.; Steinkühler, C. 2-Trifluoroacetylthiophenes, a novel series of potent and selective class II histone deacetylase inhibitors. *Bioorg. Med. Chem. Lett.* **2008**, *18*, 3456–3461.

(13) Schuetz, A.; Min, J.; Allali-Hassani, A.; Schapira, M.; Shuen, M.; Loppnau, P.; Mazitschek, R.; Kwiatkowski, N. P.; Lewis, T. A.; Maglathin, R. L.; McLean, T. H.; Bochkarev, A.; Plotnikov, A. N.; Vedadi, M.; Arrowsmith, C. H. Human HDAC7 harbors a class IIa histone deacetylase-specific zinc binding motif and cryptic deacetylase activity. *J. Biol. Chem.* **2008**, *283*, 11355–11363.

(14) (a) Somoza, J. R.; Skene, R. J.; Katz, B. A.; Mol, C.; Ho, J. D.; Jennings, A. J.; Luong, C.; Arvai, A.; Buggy, J. J.; Chi, E.; Tang, J.; Sang, B. C.; Verner, E.; Wynands, R.; Leahy, E. M.; Dougan, D. R.; Snell, G.; Navre, M.; Knuth, M. W.; Swanson, R. V.; McRee, D. E.; Tari, L. W. Structural snapshots of human HDAC8 provide insights into the class I histone deacetylases. *Structure* **2004**, *12*, 1325–1334. (b) Vannini, A.; Volpari, C.; Filocamo, G.; Casavola, E. C.; Brunetti, M.; Renzoni, D.; Charkravarty, P.; Paolini, C.; De Francesco, R.; Gallinari, P.; Steinkühler, C.; Di Marco, S. Crystal structure of a eukaryotic zinc-dependent histone deacetylase, human HDAC8, complexed with a hydroxamic acid inhibitor. *Proc. Natl. Acad. Sci. U.S.A.* **2004**, *101*, 15064–15069. (c) Vannini, A.; Volpari, C.; Gallinari, P.; Jones, P.; Mattu, M.; Carfi, A.; De Francesco, R.; Steinkühler, C.; Di Marco, S. Substrate binding to histone deacetylases as shown by the crystal structure of the HDAC8−substrate complex. *EMBO Rep.* **2007**, *8*, 879–884.

(15) Finnin, M. S.; Donigian, J. R.; Cohen, A.; Richon, V. M.; Rifkind, R. A.; Marks, P. A.; Breslow, R.; Pavletich, N. P. Structures of a histone deacetylase homologue bound to the TSA and SAHA inhibitors. *Nature (London)* **1999**, *401*, 188–193.

(16) Corminboeuf, C.; Hu, P.; Tuckerman, M. E.; Zhang, Y. Unexpected deacetylation mechanism suggested by a density functional theory QM/MM study of histone-deacetylase-like protein. *J. Am. Chem. Soc.* **2006**, *128*, 4530–4531.

(17) Yamamoto, Y.; Fujikawa, R.; Umemoto, T.; Miyaura, N. Iridium-catalyzed hydroboration of alkenes with pinacolborane. *Tetrahedron* **2004**, *60*, 10695–10700.

(18) Falck, J. R.; Kumar, P. S.; Reddy, Y. K.; Zou, G.; Capdevila, J. H. Stereospecific synthesis of EET metabolites via Suzuki−Miyaura coupling. *Tetrahedron Lett.* **2001**, *42*, 7211–7212.

(19) Nishino, N.; Shivashimpi, G. M.; Soni, P. B.; Bhuiyan, M. P. I.; Kato, T.; Maeda, S.; Nishino, T. G.; Yoshida, M. Interaction of aliphatic cap group in inhibition of histone deacetylases by cyclic tetrapeptides. *Bioorg. Med. Chem.* **2008**, *16*, 437–445.

(20) (a) Suzuki, T.; Yokozaki, H.; Kuniyasu, H.; Hayashi, K.; Naka, K.; Ono, S.; Ishikawa, T.; Tahara, E.; Yasui, W. Effect of trichostatin A on cell growth and expression of cell cycle- and apoptosis-related molecules in human gastric and oral carcinoma cell lines. *Int. J. Cancer.* **2000**, *88*, 992–997. (b) Fennell, K. A.; Miller, M. J. Synthesis of amamistatin fragments and determination of their HDAC and antitumor activity. *Org. Lett.* **2007**, *9*, 1683–1685. (c) Zhang, Y.; Adachi, M.; Zhao, X.; Kawamura, R.; Imai, K. Histone deacetylase inhibitors FK228, *N*-(2-aminophenyl)-4-[*N*-(pyridin-3-yl-methoxycarbonyl)aminomethyl]benzamide and *m*-carboxycinnamic acid bishydroxamide augment radiation-induced cell death in gastrointestinal adenocarcinoma cells. *Int. J. Cancer.* **2004**, *110*, 301–308.

(21) (a) Wittich, S.; Scherf, H.; Xie, C.; Brosch, G.; Loidl, P.; Gerhäuser, C.; Jung, M. Structure−activity relationships on phenylalanine-containing inhibitors of histone deacetylase: in vitro enzyme inhibition, induction of differentiation, and inhibition of proliferation in Friend leukemic cells. *J. Med. Chem.* **2002**, *45*, 3296–3309. (b) Remiszewski, S. W.; Sambucetti, L. C.; Atadja, P.; Bair, K. W.; Cornell, W. D.; Green, M. A.; Howell, K. L.; Jung, M.; Kwon, P.; Trogani, N.; Walker, H. Inhibitors of human histone deacetylase: synthesis and enzyme and cellular activity of straight chain hydroxamates. *J. Med. Chem.* **2002**, *45*, 753–757. (c) Belvedere, S.; Witter, D. J.; Yan, J.; Secrist, J. P.; Richon, V.; Miller, T. A. Aminosuberoyl hydroxamic acids (ASHAs): a potent new class of HDAC inhibitors. *Bioorg. Med. Chem. Lett.* **2007**, *17*, 3969–3971.

(22) The IC_{50} values for nuclear HDACs, HDAC1, and HDAC2 were used for the calculation of the potency shift value because HDAC1 and HDAC2, which are localized in the nucleus, have been reported to be important for the growth of cancer cells. (a) Lagger, G.; O'Carroll, D.; Rembold, M.; Khier, H.; Tischler, J.; Weitzer, G.; Schuettengruber, B.; Hauser, C.; Brunmeir, R.; Jenuwein, T.; Seiser, C. Essential function of histone deacetylase 1 in proliferation control and CDK inhibitor repression. *EMBO J.* **2002**, *21*, 2672–2681. (b) Huang, B. H.; Laban, M.; Leung, C. H.; Lee, L.; Lee, C. K.; Salto-Tellez, M.; Raju, G. C.; Hool, S. C. Inhibition of histone deacetylase 2 increases apoptosis and $p21^{Cip1/WAF1}$ expression, independent of histone deacetylase 1. *Cell Death Differ.* **2005**, *12*, 395–404. (c) Inoue, S.; Mai, A.; Dyer, M. J.; Cohen, G. M. Inhibition of histone deacetylase class I but not class II is critical for the sensitization of leukemic cells to tumor necrosis factor related apoptosis-inducing ligand-induced apoptosis. *Cancer Res.* **2006**, *66*, 6785–6792. (d) Witter, D. J.; Harrington, P.; Wilson, K. J.; Chenard, M.; Fleming, J. C.; Haines, B.; Kral, A. M.; Secrist, J. P.; Miller, T. A. Optimization of biaryl selective HDAC1&2 inhibitors (SHI-1:2). *Bioorg. Med. Chem. Lett.* **2008**, *18*, 726–731. (e) Methot, J. L.; Chakravarty, P. K.; Chenard, M.; Close, J.; Cruz, J. C.; Dahlberg, W. K.; Fleming, J.; Hamblett, C. L.; Hamill, J. E.; Harrington, P.; Harsch, A.; Heidebrecht, R.; Hughes, B.; Jung, J.; Kenific, C. M.; Kral, A. M.; Meinke, P. T.; Middleton, R. E.; Ozerova, N.; Sloman, D. L.; Stanton, M. G.; Szewczak, A. A.; Tyagarajan, S.; Witter, D. J.; Secrist, J. P.; Miller, T. A. Exploration of the internal cavity of histone deacetylase (HDAC) with selective HDAC1/HDAC2 inhibitors (SHI-1:2). *Bioorg. Med. Chem. Lett.* **2008**, *18*, 973–978. (f) Methot, J. L.; Hamblett, C. L.; Mampreian, D. M.; Jung, J.; Harsch, A.; Szewczak, A. A.; Dahlberg, W. K.; Middleton, R. E.; Hughes, B.; Fleming, J. C.; Wang, H.; Kral, A. M.; Ozerova, N.; Cruz, J. C.; Haines, B.; Chenard, M.; Kenific, C. M.; Secrist, J. P.; Miller, T. A. SAR profiles of spirocyclic nicotinamide derived selective HDAC1/HDAC2 inhibitors (SHI-1:2). *Bioorg. Med. Chem. Lett.* **2008**, *18*, 6104–6109. (g) Zhou, N.; Moradei, O.; Raeppel, S.; Leit, S.; Frechette, S.; Gaudette, F.; Paquin, I.; Bernstein, N.; Bouchain, G.; Vaisburg, A.; Jin, Z.; Gillespie, J.; Wang, J.; Fournel, M.; Yan, P. T.; Tranchy-Bourget, M. C.; Kalita, A.; Lu, A.; Rahil, J.; MacLeod, A. R.; Li, Z.; Besterman, J. M.; Delorme, D. Discovery of *N*-(2-aminophenyl)-4-[(4-pyridin-3-ylpyrimidin-2-ylamino)methyl]benzamide (MGCD0103), an orally active histone deacetylase inhibitor. *J. Med. Chem.* **2008**, *51*, 4072–4075.

(23) (a) Hubbert, C.; Guardiola, A.; Shao, R.; Kawaguchi, Y.; Ito, A.; Nixon, A.; Yoshida, M.; Wang, X.-F.; Yao, T.-P. HDAC6 is a microtubule-associated deacetylase. *Nature (London)* **2002**, *417*, 455–458. (b) Matsuyama, A.; Shimazu, T.; Sumida, Y.; Saito, A.; Yoshimatsu, Y.; Seigneurin-Berny, D.; Osada, H.; Komatsu, Y.; Nishino, N.; Khochbin, S.; Horinouchi, S.; Yoshida, M. In vivo destabilization of dynamic microtubules by HDAC6-mediated deacetylation. *EMBO J.* **2002**, *21*, 6820–6831.

(24) (a) Philipp, M.; Bender, M. L. Inhibition of serine proteases by arylboronic acid. *Proc. Natl. Acad. Sci. U.S.A.* **1971**, *68*, 478–480. (b) Flentke, G. R.; Munoz, E.; Huber, B. T.; Plaut, A. G.; Kettner, C. A.; Bachovchin, W. W. Inhibition of dipeptidyl aminopeptidase IV (DP-IV) by Xaa-boroPro dipeptides and use of the these inhibitors to examine the role of DP-IV in T-cell function. *Proc. Natl. Acad. Sci. U.S.A.* **1991**, *88*, 1556–1559.

(25) Kim, N. N.; Cox, J. D.; Baggio, R. F.; Emig, F. A.; Mistry, S. K.; Harper, S. L.; Speicher, D. W.; Morris, S. M., Jr.; Ash, D. E.; Traish, A.; Christiason, D. W. Probing erectile function: *S*-(2-boronoethyl)-L-cysteine binds to arginase as a transition state analogue and enhances smooth muscle relaxation in human penile corpus cavernosum. *Biochemistry* **2001**, *40*, 2678–2688.

(26) (a) Adams, J.; Behnke, M.; Chen, S.; Cruickshank, A. A.; Dick, L. R.; Grenier, L.; Klunder, J. M.; Ma, Y.-T.; Plamondon, L.; Stein, R. L. Potent and selective inhibitors of the proteasome: dipeptidyl boronic acid. *Bioorg. Med. Chem. Lett.* **1998**, *8*, 333–338. (b) Adams, J.; Palombella, V. J.; Sausville, E. A.; Johnson, J.; Destree, A.; Lazarus, D. D.; Maas, J.; Pien, C.; S.; Prakash, S.; Elliott, P. J. Proteasome inhibitors: a novel class of potent and effective antitumor agents. *Cancer Res.* **1999**, *59*, 2615–2622.

(27) (a) Monks, A.; Scudiero, D.; Skehan, P.; Shoemaker, R.; Paull, K.; Vistica, D.; Hose, C.; Langley, J.; Cronise, P.; Vaigro-Wolff, A.; Gray-Goodrichi, M.; Campbell, H.; Mayo, J.; Boyd, M. R. Feasibility of a high-flux anticancer drug screen using a diverse panel of cultured human tumor cell lines. *J. Natl. Cancer Inst.* **1991**, *83*, 757–766. (b) Yamori, T.; Sato, S.; Chikazawa, H.; Kadota, T. Anti-tumor efficacy of paclitaxel against human lung cancer xenografts. *Jpn. J. Cancer*

Res. **1997**, *88*, 1205–1210. (c) Yamori, T.; Matsunaga, A.; Sato, S.; Yamazaki, K.; Komi, A.; Ishizu, K.; Mita, I.; Edatsugi, H.; Matsuba, Y.; Takezawa, K.; Nakanishi, O.; Kohno, H.; Nakajima, Y.; Komatsu, H.; Andoh, T.; Tsuruo, T. Potent antitumor activity of MS-247, a novel DNA minor groove binder, evaluated by an in vitro and in vivo human cancer cell line panel. *Cancer Res.* **1999**, *59*, 4042–4049. (d) Yaguchi, S.; Fukui, Y.; Koshimizu, I.; Yoshimi, H.; Matsuno, T.; Gouda, H.; Hirono, S.; Yamazaki, K.; Yamori, T. Antitumor activity of ZSTK474, a new phosphatidylinositol 3-kinase inhibitor. *J. Natl. Cancer Inst.* **2006**, *98*, 545–556. (e) Dan, S.; Tsunoda, T.; Kitahara, O.; Yanagawa, R.; Zembutsu, H.; Katagiri, T.; Yamazaki, K.; Nakamura, Y.; Yamori, T. An integrated database of chemosensitivity to 55 anticancer drugs and gene expression profiles of 39 human cancer cell lines. *Cancer Res.* **2002**, *62*, 1139–1147.

(28) Skehan, P.; Storeng, R.; Scudiero, D.; Monks, A.; McMahon, J.; Vistica, D.; Warren, J. T.; Bokesch, H.; Kenney, S.; Boyd, M. R. New colorimetric cytotoxicity assay for anticancer-drug screening. *J. Natl. Cancer Inst.* **1990**, *82*, 1107–1112.

JM900125M